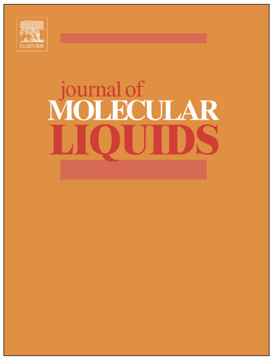

Experimental and computational studies on hydroxamic acids as environmental friendly chelating corrosion inhibitors for mild steel in aqueous acidic medium

Dakeshwar Kumar Verma, Akram Al Fantazi, Chandrabhan Verma, Fahmida Khan, Ashish Asatkar, Chaudhery Mustansar Hussain, Eno E. Ebenso

PII: S0167-7322(20)32502-2
DOI: https://doi.org/10.1016/j.molliq.2020.113651
Reference: MOLLIQ 113651

To appear in: *Journal of Molecular Liquids*

Received date: 21 April 2020
Revised date: 14 June 2020
Accepted date: 19 June 2020

Please cite this article as: D.K. Verma, A. Al Fantazi, C. Verma, et al., Experimental and computational studies on hydroxamic acids as environmental friendly chelating corrosion inhibitors for mild steel in aqueous acidic medium, *Journal of Molecular Liquids* (2020), https://doi.org/10.1016/j.molliq.2020.113651

Experimental and computational studies on hydroxamic acids as environmental friendly chelating corrosion inhibitors for mild steel in aqueous acidic medium

Dakeshwar Kumar Verma[a], Akram Al Fantazi[b], Chandrabhan Verma[c]*, Fahmida Khan[d], Ashish Asatkar[e], Chaudhery Mustansar Hussain[f] and Eno E. Ebenso[g]*

[a]*Department of Chemistry, Govt. Digvijay Autonomous Postgraduate College, Rajnandgaon, Chhattisgarh, INDIA, 491441*
[b]*Department of Chemical Engineering, Khalifa University of Science and Technology, P.O. Box 2533, Abu Dhabi, United Arab Emirates*
[c]*Center of Research Excellence in Corrosion, Research Institute, King Fahd University of Petroleum and Minerals, Dhahran 31261, Saudi Arabia*
[d]*Department of Chemistry, National Institute of Technology Raipur, Raipur 492010, CG, India*
[e]*Department of Chemistry, Govt. Gundadhur Postgraduate College, Kondagaon, Chhattisgarh, INDIA*
[f] *Department of Chemistry and Environmental Science, New Jersey Institute of Technology, Newark, N J 07102, USA*
[g]*Department of Chemistry, School of Chemical and Physical Sciences and Material Science Innovation & Modelling (MaSIM) Research Focus Area, Faculty of Natural and Agricultural Sciences, North-West University, Private Bag X2046, Mmabatho 2735, South Africa*

Corresponding Address: *chandraverma.rs.apc@itbhu.ac.in* (CV) & Eno.Ebenso@nwu.ac.za (EEE)

GRAPHICAL ABSTRACT

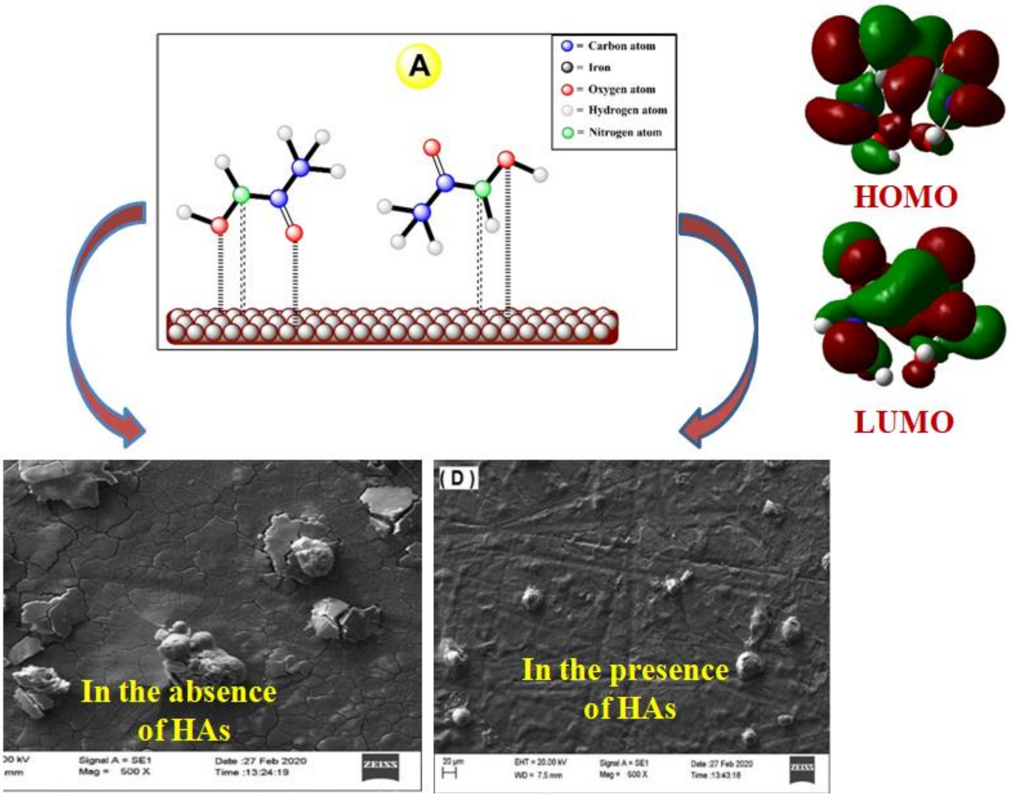

ABSTRACT

In the present study, three hydroxamic acids (HAs) namely acetohydroxamic acid (AHA), benzohydroxamic acid (BHA) and oxalohydroxamic acid (OHA) synthesised, characterized and used as inhibitors for mild steel corrosion in the electrolytic solution of 1M HCl. Corrosion inhibition property of HAs was evaluated using several chemical, electrochemical, surface and computational methods. Results showed that studies HAs act as effective corrosion inhibitors and their inhibition efficiencies follow the order: OHA (96.37%) > BHA (95.69%) > AHA (93.29%). EIS study showed that studied HAs act as interface type inhibitors. Polarization study revealed that HAs demonstrate themselves as mixed type corrosion inhibitors and they adsorb on the active sites of metallic surface. Adsorption of HAs on metal-1M HCl interfaces followed the Langmuir adsorption isotherm model. Surface morphological analyses of inhibited and uninhibited metallic surface were carried out using SEM-EDX and XRD methods. DFT analyses showed that studied compounds act as chelating type of ligands. Effect of Keto-enol tautomerism and different possible conformational isomers on metallic corrosion inhibition was demonstrated. The conformational isomers in which >C=O and –OH (hydroxyl) groups present in same side behave as chelating ligands and form relatively more stable complex than that of conformational isomers in which >C=O and –OH groups present in opposite side. Experimental and DFT studies well complimented each other.

Keywords: Tautomers as corrosion inhibitors, conformational isomers, chelating corrosion inhibitors, Hydroxamic acid and Langmuir adsorption isotherm.

1. Introduction

Corrosion is a process in which metallic materials undergo degradation through chemical and/ or electrochemical reactions with the components of the surrounding environment. Corrosion is a natural and spontaneous process in which a pure metal converts in to its relatively more stable oxide, chloride, carbonate and sulphate etc. Though, complete prevention of metallic corrosion is practically impossible however the rate of corrosive dissolution and its adverse effect can be minimized using previously used methods of corrosion mitigation such as alloying, dealloying, coatings, paintings, passivation and corrosion inhibitors [1-4]. Basic requirements for a compound to be used as corrosion inhibitor are shown in Fig.1. Use of synthetic corrosion inhibitors is one of the most effective methods because of their ease of synthesis and high inhibition effectiveness. Most of the well-know corrosion inhibitors are heteroatoms (N, O, P, and S) and aromatic rings containing compounds. Obviously, polar functional groups such as –OH, –OMe, $–NH_2$, –NH–, –COOH, –CN, –O–, $–NO_2$, $–CONH_2$, $–COOC_2H_5$ and –N=N– etc. [5-12] enhance the solubility of organic inhibitors in polar electrolytes. Heteroatoms of the polar functional groups also act as adsorption centers as they can transfer their non-bonding electrons to the metallic d-orbitals through coordination boding [13-15]. Along with non-bonding electrons of heteroatoms, multiple bonds of aromatic rings and side chain also favour the adsorption of organic inhibitors on metallic surface through dπ-pπ bonding type of interactions. Problem of the corrosive dissolution is even more severe during acid cleanings of metallic ores that acquire the implementation of aggressive solutions such as HCl, H_2SO_4, HNO_3, NaCl and H_3PO_4 etc. Some of the common industrial cleaning processes are acid pickling, descaling, acid descaling and oil-well acidification [15-20].

Hydroxamic acids (HAs) represent a special class of organic compounds that possess several biological and industrial applications. Hydroxamic acid and its derivatives are reported as potential biological agents toward anti-asthmatic and anti-inflammatory activities [21]. Additionally, HAs form highly stable complexes with transition metal cations due to the presence of several electron rich (donor) oxygen and nitrogen heteroatoms. The HAs can be regarded as chelating ligands as they possess at least two electron rich sites (non-bonding and/or π-electrons) that can form coordination bondings with the metallic d-orbitals [22,23]. Because of their high complexation ability, HAs are expected to possess high adsorption tendency on metallic surface. Therefore, HAs can be used as one of the best alternatives to traditional existing corrosion inhibitors that generally show low efficiency at relatively high concentration. In view of this, some of the authors recently reported the corrosion inhibition effect of hydroxamic acids [24, 25]. Because of their natural and biological activities, HAs can be regarded as green and environmental friendly alternatives to the traditional toxic corrosion inhibitors.

Herein, three hydroxamic acids (HAs) designated as AHA, BHA and OHA are used as corrosion inhibitors for mild steel in 1 M HCl medium. Inhibition efficiencies of the HAs were measured using chemical (weight loss), electrochemical (EIS and PDP), surface (SEM and EDX) and density functional theory (DFT) methods. All the studied HAs showed reasonably good protection efficiencies for mild steel in 1M HCl. DFT study is also carried out to demonstrate the effect of different tautomeric forms o tested HAs on their protection capability. Generally, HAs are represented as RC(O)N(OH)R' and different conformational isomers can be constructed for three studied HAs based on the orientation of R and R'. DFT study was also performed for different conformations isomers of investigated HAs to demonstrate the effect of relative orientation of different groups on the corrosion inhibition performance. Outcomes of the study revealed that AHA, BHA and OHA act as chelating ligands and form stable complexes with metallic surface. Protection efficiency of the tested compounds was first of all investigated using weight loss method and supported by electrochemical studies using potentiodynamic polarization and electrochemical impedance spectroscopic methods. Surface morphology studies and adsorption behaviour of investigated compounds was determined using SEM-EDS and XRD methods. DFT study was undertaken in order to describe the nature metal-inhibitor interactions. DFT study also carried out to demonstrate the effect of different tautomers and conformational isomers of AHA, BHA and OHA on MS corrosion in 1M HCl. Several experimental and computational indices were computed and described. The order of protection efficiencies of tested HAs derived from chemical, electrochemical and surface investigations were well complimented by DFT studies.

2. Methods and Materials

2.1. Synthesis of HAs

Acetohydroxamic acid (AHA) was synthesized as per the previously used method [26]. In brief, 15 ml double distilled water, 12 ml ethanol and 7g crystalline hydroxylamine hydrochloride were taken in a 500 ml round bottom flask. The mixture was allowed to stir until the above reaction mixture becomes clear. After that, 20 ml of sodium hydroxide (10 mol/L) was added slowly. Temperature of the reaction mixture was maintained at 20°C. In the above reaction mixture, ethyl acetate (0.1 mol) added gradually at room temperature and kept in ice bath for cooling. To the above reaction mixture concentrated HCl was added to decrease the pH level up to 6. After that, 100 ml ethanol was added to above reaction mixture to get yellow colored precipitate. The precipitate was dissolved in a mixture of ethyl acetate and acetone. After proper dissolution, the above reaction mixture cooled to room temperature and kept overnight in freezer to get white crystals of acetohydroxamic. AHA showed the melting point of 88°C±1. Similarly, BHA was prepared using the protocol described previously [26]. 1.4 of hydroxylamine hydrochloride and 2.1 g sodium carbonate (anhydrous) were dissolved in 50 ml ether. Above reaction was stirred to get a homogeneous reaction mixture using a magnetic stirrer. At constant stirring, 2.8 g benzoyl chloride and 3.5 ml double distilled water were added slowly. The above reaction mixture was stirred for 30 minute. The residual solvents (mainly ether) were removed using rotatory evaporator and resultant mixture was kept overnight to get crystalline raw material. Finally, crystallization of the above crude material with ethyl acetate results in to the formation of pure BHA having the melting point of 128°C ±1. For OHA synthesis, 9.0 g of hydroxylamine hydrochloride and 7.1 g of diethyl oxalate were added drop-wise with proper shaking at 0°C for 25-30 minutes. The precipitate of raw OHA was obtained after some time that was crystallized in double distilled water to give pure OHA having melting point of 161°C ±1[24]. The chemical structure, IUPAC name, abbreviations, and FT-IR, 1H and 13C NMR characterization data of investigated HAs are reported in Table 1 and their respective spectra are shown in Fig. S1.

2.2. *Test material and electrolyte*

Mild steel sheet having chemical composition of (%) C = 0.18, O = 0.08, S = 0.06, P = 0.04, Cr = 0.04 and reminder Fe was used for the preparation of test specimens for weight loss, electrochemical and surface analyses. The metallic specimens were abraded using emery papers of different (400-1200) grades, washed (with water), and degreased with acetone. The analytical grade HCl (37% HCl MERCK) was used for the preparation of test electrolyte of 1 M HCl electrolytic. Protection efficiency of HAs was determined at their different concentrations ranging from 20-80 ppm.

2.3. *Weight loss measurement*

Weight loss or gravimetric study is one of most simple, reliable, effective, reproducible, and cost-effective methods for the determination of inhibition efficiency of corrosion inhibitors that does not require employment of any tedious process and expensive instruments. Several useful indices including corrosion rate (ρ), surface coverage (θ) and inhibition efficiency (%η) can be derived using weight loss experimentation. Using weight loss technique, protection efficiency of HAs was measured at their different concentrations in the temperature range of 298–328 K. The weight loss tests were performed for the immersion time of 6h. Weight loss experiments (at each concentration) were triply performed and maximum observed standard derivations were less than 2%. The corrosion rates (ρ) values for mild steel corrosion in acidic medium were calculated using the following equation [27]:

$$\rho = \frac{\Delta w}{At} (1)$$

where, ΔW, A and t represent the weight loss (in mg), the metallic surface area (in cm^2) and immersion time (6h), respectively. Using corrosion rate (ρ) values, the inhibition efficiency ($\%\eta$) was evaluated using following equation [27]:

$$\%\eta = \left(\frac{\rho^1-\rho^2}{\rho^1}\right) \times 100 \qquad (2)$$

Where ρ^1 and ρ^2 represent the corrosion rate values for mild steel corrosion in 1M HCl with and without HAs, respectively.

2.4. Electrochemical analyses

Potentiostat Gamry Echem Analyst 5.0 Software G- 300 model was applied for electrochemical studies. The instrument consists of platinum as a counter electrode, mild steel as a working electrode and SCE as a reference electrode. The electrochemical studies were performed after immersing the MS in 1M HCl for 30 minute in order to get open circuit potential (OCP) established. For EIS study, an AC signal of 10 mV amplitude in the frequency range of 100 kHz-0.01 mHz was employed. The Nyquist curves for MS corrosion were fitted in suitable equivalent circuit (Fig. 6). The equivalent circuit consists of solution resistance (R_s), a charge transfer resistance (R_{ct}) and a constant phase element. The values of charge transfer resistance and inhibition efficiency ($\%\eta$) at different concentrations of HAs were derived using following equation [28]:

$$\%\eta = \frac{R_{ct\,(inh)}-R_{ct}}{R_{ct\,(inh)}} \times 100 \qquad (3)$$

In above equation, $R_{ct(inh)}$ and R_{ct} represent the charge transfer resistances for MS corrosion with and without HAs, respectively. For polarization studies, MS potential allowed to scan in the potential range of -250 to +250 V at the constant scan rate of 1 mV s^{-1} (with respect to the potential of SCE) [21]. The obtained anodic and cathodic Tafel curves were extrapolated to get the values of corrosion current densities (i_{corr}) through which inhibition efficiencies ($\%\eta$) at several concentrations of HAs were calculated using following relationship [29]:

$$\%\eta = \frac{i_{corr}-i_{corr(inh)}}{i_{corr}} \text{ x } 100 \qquad (4)$$

where, i_{corr} and $i_{corr\ (inh)}$, represent the values of corrosion current densities for MS corrosion in 1M HCl without and with HAs, respectively.

2.5. SEM-EDS and XRD studies

The scanning electron microscope (SEM) coupled with electron dispersion X-ray spectroscopy (EDS) analyses were carried out to support the electrochemical studies. For

SEM-EDX analyses, MS surfaces are allowed to corrode freely in test electrolyte (1M HCl) in the absence and presence of 80 ppm concentration of HAs. After 6h immersion time, surfaces of the corroded specimens were examined using SEM-EDX methods. The ZEISS EVO SEM 18 / INCA 250 EDS XMAX with a detector (20mm) Oxford model was employed for SEM-EDS analyses. X-ray diffraction (XRD) analysis was carried out to determine the nature of protective layer deposited on the surface of metal. The stretch samples collected from the inhibited (80 ppm) and uninhibited metallic surfaces were used for XRD analysis. The PAN Analytical, Netherland X-ray diffractometer was used for this purpose.

2.6. DFT analyses

Density function theory (DFT) based quantum chemical calculations were performed to support the experimental studies. Recently, DFT has emerged one of the most powerful techniques to demonstrate the interactions between corrosion inhibitors and metallic surfaces. In the present study, interactions of HAs and MS surface were demonstrated using Gaussian 09 and basis set of G-31 + G (d, p) basic. The DFT studies were performed on different possible tautomeric and conformational isomers of HAs. Using DFT studies, energies of frontier molecular orbital pictures (E_{HOMO} and E_{LUMO}) and different related indices were derived using following relationships [30]:

$$IE = -E_{HOMO} \qquad (5)$$

$$EA = -E_{LUMO} \qquad (6)$$

$$\eta = \frac{1}{2}(IE - EA) = \frac{1}{2}(-E_{HOMO} + E_{LUMO}) \qquad (7)$$

$$\sigma = \frac{1}{\eta} \qquad (8)$$

$$\chi = \frac{1}{2}(IE + EA) = \frac{1}{2}(-E_{HOMO} - E_{LUMO}) \qquad (9)$$

$$\Delta N = \frac{\chi_{Fe} - \chi_{inh}}{2(\eta_{Fe} + \eta_{inh})} \qquad (10)$$

For the calculation of ΔN (fraction of electron transfer) values, work function of iron (4.88 eV) was used instead of electronegativity of iron. The lowest energy crystalline iron (110) surface was selected for fraction of electron transfer (ΔN_{110}) calculation.

3. Result and discussion

3.1. Weight loss measurements

Effect of AHA, BHA and OHA concentration on MS corrosion in 1M HCl at the different temperatures is presented in Table 2. It can be clearly seen that protection efficiency of AHA, BHA and OHA increases with increasing their concentrations and maximum increase was observed at 80 ppm concentration. Obviously, increase in the AHA, BHA and OHA concentration results consecutive raise in the surface coverage that result in to the corresponding increase in their protection efficiency. Inhibition efficiencies of the HAs followed the order: OHA (96.37%)> BHA (95.69%)> AHA (93.29%). Difference in protection efficiencies of AHA, BHA and OHA can be explained on the basis of their molecular structures. The higher protection efficiency of BHA as compared to AHA can be explained on the basis of the presence of aromatic (phenyl) moiety instead of methyl group of the AHA. Presence of three additional double bonds of the aromatic ring enhances the effectiveness of BHA adsorption on MS surface due to dπ-πp interactions. OHA contains additional -CO-NH-OH moiety at the place of phenyl ring of BHA. The -CO-NH-OH of OHA should be considered as more electron donor as compared to the aromatic ring of BHA as former contains two oxygen and one nitrogen atoms and one double bond in the form of carbonyl group that can form more strong complex with metallic d-orbital than that of the three double bonds of latter. Careful observation (Table 2) showed that protection efficiencies of the AHA, BHA and OHA decrease on increasing the temperature. Increase in temperature may results into the fractionation, arrangement or/ and decomposition of the HAs molecules that can adversely affect their protection power. More so, increase in kinetic energy of the HAs at elevated temperature can also decrease the adsorption abilities of AHA, BHA and OHA molecules [31].

3.2. Adsorption isotherm

Adsorption isotherm analysis is one of the most important aspects of metal-corrosion interactions. Langmuir adsorption isotherm is the most common and frequently used isotherm models that can be presented using following relationship [32]:

$\frac{C}{\theta} = \frac{1}{K_{ads}} + C$ (11)

where, K_{ads} represent adsorption-desorption constant. In the present study, Langmuir adsorption isotherm model was well fitted with correlation coefficient (R^2) values close to unity. Using K_{ads} values, the standard free energy of adsorption (ΔG_{ads}) values were calculated using following equation [32]:

$\Delta G_{ads} = -RT \ln (55.5\ K\text{ads})$ (12)

Here, numerical value of 55.5 denotes the molar concentration of water and R is the gas constant and T represents the absolute temperature.The values of K_{ads} and ΔG_{ads} at different studied temperatures are presented in Table 3. High numerical values of K_{ads} showed that AHA, BHA and OHA have strong ability to adsorb on metallic surface. Negative values of ΔG_{ads} revealed that AHA, BHA and OHA spontaneously adsorb on metallic surface using their electron rich centers. Literature survey reveals that ΔG_{ads} value of -40 kJ mol^{-1} or more negative is consisted with chemisorption while its value of -20 kJ mol^{-1} or less negative is consistent with physisorption mechanism [25,26]. Results presented in Table 3 showed that adsorption of the AHA, BHA and OHA on MS surface obeyed the physiochemisorption by means of minor supremacy of physisorption mechanism as values of ΔG_{ads} for AHA, BHA and OHA are more close to -20 kJ/mol as compared to the -40 kJ/mol[33-34].

3.3. Electrochemical analysis

3.2.1. Potentiodynamic Polarization (PDP)

Anodic and cathodic Tafel curves for MS corrosion in 1M HCl with and without AHA, BHA and OHA at their different concentrations (40 - 80 ppm) are shown in Fig. 3 (a-c) and various PDP parameters such as inhibition efficiency (%η), corrosion potential (E_{corr}), corrosion current density (i_{corr}), cathodic (β_c) and anodic (β_a) Tafel slopes are summarized in Table 4. From Fig.3 it can clearly seen that shape of anodic and cathodic curves are significantly affected in the presence of AHA, BHA and OHA indicating that they exert remarkable anticorrosion effect on both anodic and cathodic reactions [35,36]. More so, careful observation of the results presented in table 4 showed that corrosion current density values are much lower in the presence of AHA, BHA and OHA than that of in their absence. This observation suggests that AHA, BHA and OHA effectively adsorb on the metallic surface using their electron rich centers and block the active sites responsible for the corrosion [35-

36]. Observation of the results also showed that presence of AHA, BHA and OHA did not cause any significant shift in the value of corrosion potential (E_{corr}) indicating that AHA, BHA and OHA act as mixed type inhibitors [37-39]. The order of protection efficiencies of AHA, BHA and OHA derived from PDP study was consistent with the order of protection efficiency derived using weight loss method.

3.2.2. Electrochemical impedance spectroscopy (EIS)

EIS is one of the most important electrochemical methods to demonstrate the interfacial behaviours of corrosion inhibitors. Nyquist plots for MS corrosion in 1 M HCl at different AHA, BHA, and OHA concentrations are shown in Fig. 4 (a-c). Nyquist plots represent a single semicircle indicating that MS corrosion with and without AHA, BHA and OHA involve a single charge transfer (SCT) mechanism. The SCT mechanism of MS corrosion in 1M HCl with and without AHA, BHA and OHA was further reinforced by single maxima in the Bode plots (Fig.5). Increase in the diameter of the Nyquist curves on increasing the AHA, BHA and OHA concentration is attributed to the increase in the value of charge transfer resistance due to AHA, BHA and OHA adsorption at the MS-1M HCl interfaces. This finding suggests that AHA, BHA and OHA act as interface type inhibitors and their presence results in to formation of protective film at metal-electrolyte interfaces [40]. Equivalent circuit used for fitting of Nyquist curves is presented in Fig. 6[41]. The double-layer capacitance (C_{dl}) for MS corrosion can be presented as follows [42]:

$$C_{dl} = Yo(\omega_{max})^{n-1} \quad (13)$$

where, n and Y_0 represent the phase shift and exponent, respectively. ω represents the angular frequency. Different EIS parameters are summarized in Table 5. Increase in the value of R_{ct} and decrease in the values of C_{dl} is attributed to the adsorption of AHA, BHA and OHA on metallic surface and increase in the thickness of electric double layer, respectively [43-45].

3.4. SEM-EDS analyses

SEM images and EDX spectra of MS surfaces corroded in 1M HCl with and without AHA, BHA and OHA are shown Fig. 7 (a-d) and Fig. 8 (a-d), respectively. It can be clearly seen that morphology of the MS surfaces are much smoother in the presence of AHA, BHA and OHA than that of in their absence. This observation reveals that AHA, BHA and OHA adsorb on metallic surface and protect from corrosive degradation. The adsorption of the AHA, BHA and OHA on MS surface was further supported by EDX spectral analyses. Increase in the intensity of EDX signal for oxygen and presence of additional signals for heteroatoms (Table 6) in the presence of AHA, BHA and OHA validate the adsorption mechanism of corrosion inhibition.

3.5. X-ray diffraction (XRD) analysis

Recently, XRD has immersed as one of the potential tool for the identification of crystalline phase and to identify the nature of protective layer deposited onto metallic surface. Fig. 9 represents the XRD patterns of the inhibited and uninhibited scratched samples. Fig. 9a depicts the XRD pattern of scratched sample of mild steel surface in the presence of 1 M HCl. The XRD pattern shows three peaks at 2θ = 37.2°, 43.5°, 44.7° and 54.8° which is resulted due to deposition of surface metallic oxides (Fe_3O_4 and FeOOH) [31, 46]. Careful observation (Fig. 9b-d) showed that XRD patterns of the scratched samples containing AHA, BHA and OHA showed XRD peaks of little intensities. The decrease in intensities of XRD patterns indicates the non-crystalline nature of deposit protective oxide layers.

3.6. Quantum chemical calculations

DFT based quantum chemical calculation is one of the most significant and frequently used computational methods to demonstrate the adsorption and interaction behaviour of corrosion inhibitors [47-50]. Recall that several DFT based parameters such as E_{LUMO} (Lowest Occupied Molecular Orbital), E_{HOMO} (Highest Unoccupied Molecular Orbital), dipole moment (μ), energy gap (ΔE), electron transfer fraction (ΔN), global hardness (η) and electronegativity (χ) are computed from the keto and enol forms and some of the major conformational isotherms of AHA, BHA and OHA and are presented in Table 7. From the frontier molecular orbital picture it can be seen that HOMO and LUMO are localized over the entire parts of the AHA, BHA and OHA molecules. This observation suggests that they act as strong electron donor as well as strong electron acceptor. Obviously, HOMO defines the part of inhibitor molecules responsible for electron donation and a higher value of E_{HOMO} is consistent with high electron donating ability. Conversely, LUMO defines the part of inhibitor molecules responsible for electron acceptance and a lower value of E_{LUMO} is consistent with high electron accepting ability [51, 52]. Careful observation of the results presented in Table 7 showed that AHA, BHA and OHA are associated with relatively high values of E_{HOMO} and lower values of E_{LUMO} therefore they offer strong donor-acceptor interactions with the metallic surface and act as effective corrosion inhibitors[53]. Frontier molecular orbital pictures (HOMO and LUMO) for AHA, BHA and OHA are shown in Figs.

10-12. DFT studies were carried out for keto and enol forms of the AHA, BHA and OHA molecules along with some common conformational isomers. Different conformational isomers are constructed based on the orientation of hydroxyl (-OH) attached with nitrogen with respect to the carbonyl (>C=O) functional group as presented in Figs. 10-12.

It is important to mention that C-N bond of AHA Keto-I acquires the bond length of 1.37Å which is relatively lesser as compared to the normal C-N bond length. The reduction in the C-N bond length is might be due to resonance between carbonyl (>C=O) functional group and unshared pair electrons of nitrogen. Intermolecular H-bonding between >C=O (carbonyl) and –OH (hydroxyl) groups can also plays a significant role in the reduction of C-N bond length. The H-bond length in Keto-I form (AHA) was 1.96Å. In AHA Keto-II form (>C=O and –OH present in the opposite side), observed C-N bond length was 1.40 Å. Similarly, C-N and H-bonding acquire the bond lengths of 1.38 Å and 1.93 Å, respectively.

The OHA has two hydroxamic acid groups therefore theoretically three major conformational isomers are possible as presented in Fig. 12. It important to notice that AHA, BHA and OHA in their keto and enol forms do not show any remarkable change in the DFT parameters. Similarly, different conformational isomers also did not show any remarkable change in their values of DFT indices. However, careful observation of the DFT results presented in Table 7 showed that conformational isomeric forms of AHA, BHA and OHA in which >C=O and –OH (hydroxyl) groups present in same side are more effective corrosion inhibitors than that of their enol-tautomeric forms. This can be explained on the basis of complexation behaviour of AHA, BHA and OHA with metallic d-orbital. Obviously, in keto-tautomeric form in which >C=O and –OH (hydroxyl) groups present in same side behave as chelating ligands and form relatively more stable complex than that of the conformational isomeric forms of AHA, BHA and OHA in which >C=O and –OH groups present in opposite side.

3.7. Corrosion inhibition mechanism

It is well established that most of the organic compounds interact with metallic surface using donor-acceptor or charge sharing mechanism. Mostly, they interact with physiochemisorption mechanism. Physisorption is mostly occurs via the interaction between charge metallic surface charged inhibitor molecules whereas chemisorption takes place through charge sharing between metallic orbitals and inhibitor molecules. Several factors including temperature, nature of metal and electrolyte, immersion time etc. affect the adsorption behaviour of the inhibitor molecules. Nevertheless, adsorption of inhibitor molecules results into the formation inhibitive films that isolate the metal from corrosive environment [54]. It is established that in acidic medium, adsorption of organic inhibitors containing heteroatoms in their molecular structures proceeds through physisorption and finally chemisorption. The compounds tested as corrosion inhibitors in the present study contain numerous electron rich centers through which they can effectively adsorb and inhibit metallic corrosion. These electron rich centers transfer their non-bonding and π-electrons into surface metallic orbital and form coordination bondings [55,56]. The adsorption behaviour of different tested corrosion inhibitors is illustrated in Fig. 13.

4. Conclusions

In the present study, corrosion inhibition effect of three hydroxamic acids namely acetohydroxamic acid (AHA), benzohydroxamic acid (BHA) and oxalohydroxamic acid (OHA) for mild steel corrosion is evaluated using chemical, electrochemical, surface and DFT methods. Following conclusions were drawn:

1. AHA, BHA and OHA act as effective corrosion inhibitors for mild steel in 1M HCl
2. Their effectiveness followed the order: OHA (96.37%)> BHA (95.69%)> AHA (93.29%).
3. Potentiodynamic polarization study showed that AHA, BHA and OHA behaved as mixed type corrosion inhibitors.
4. EIS study showed that AHA, BHA and OHA behaved as interface type.
5. Adsorption of AHA, BHA and OHA at the interface of MS and 1M HCl obeyed the Langmuir adsorption isotherm model.
6. DFT study suggests that AHA, BHA and OHA interact with donor-acceptor interactions.
7. In conformational isomeric forms of AHA, BHA and OHA in which >C=O and –OH (hydroxyl) groups present in same side behave as chelating ligands.

Acknowledgements

Author Dr. Dakeshwar Kumar Verma thankful to principal govt. Digvijay College for providing instrumental and basic facilities

5. Conflict of interest

Authors declared no conflict of interest

References

1. Singh, A., Ansari, K. R., Quraishi, M. A., Kaya, S. and Banerjee, P. The effect of an N-heterocyclic compound on corrosion inhibition of J55 steel in sweet corrosive medium, New Journal of Chemistry, 43 (2019)6303-6313.
2. Verma, C., Olasunkanmi, L.,Ebenso, E.E., & Quraishi, M.A., C. Verma, L. Olasunkanmi, E.E. Ebenso,M. Quraishi, Substituents effect on corrosion inhibition performance of organic compounds in aggressive ionic solutions: a review, Journal of Molecular Liquids, 251 (2017) 100–118.
3. Dehghani, A., Bahlakeh, G., Ramezanzadeh, B. and Ramezanzadeh, M.Potential role of a novel green eco-friendly inhibitor in corrosion inhibition of mild steel in HCl solution: Detailed macro/micro-scale experimental and computational explorations, Construction and Building Materials, 245 (2020) 118464.
4. Verma, C., Verma, D.K., Ebenso, E.E., & Quraishi, M.A., (2018). Sulfur and phosphorus heteroatom-containing compounds as corrosion inhibitors: An overview. Heteroatom Chemistry, e21437.
5. Solomon, M. M., Umoren, S. A., Quraishi, M. A., & Salman, M. (2019). Myristic acid based imidazoline derivative as effective corrosion inhibitor for steel in 15% HCl medium. Journal of Colloid and Interface Science, 551, 47–60. https://doi.org/10.1016/j.jcis.2019.05.004
6. Zhang, J. (2020). 2-(3H-Imidazol-4-yl)-ethylamine as a green corrosion inhibitor for Q235 steel in hydrochloric acid. International Journal of Electrochemical Science, 15(2), 1437–1449. https://doi.org/10.20964/2020.02.27.
7. Singh, A., Ansari, K. R., Haque, J., Dohare, P., Lgaz, H., Salghi, R., & Quraishi, M. A. (2018). Effect of electron donating functional groups on corrosion inhibition of mild steel in hydrochloric acid: Experimental and quantum chemical study. Journal of the Taiwan Institute of Chemical Engineers, 82, 233–251. https://doi.org/10.1016/j.jtice.2017.09.021.
8. Salarvand, Z., Amirnasr, M., Talebian, M., Raeissi, K., & Meghdadi, S. (2017). Enhanced corrosion resistance of mild steel in 1 M HCl solution by trace amount of 2-phenyl-benzothiazole derivatives: Experimental, quantum chemical calculations and molecular dynamics (MD) simulation studies. Corrosion Science, 114, 133–145. https://doi.org/10.1016/j.corsci.2016.11.002.

9. El Aoufir, Y., Lgaz, H., Bourazmi, H., Kerroum, Y., Ramli, Y., Guenbour, A., &Oudda, H. (2016). Quinoxaline derivatives as corrosion inhibitors of carbon steel in hydrochloridric acid media: Electrochemical, DFT and montecarlo simulations studies. Journal of Materials and Environmental Science, 7(12), 4330–4347.
10. Obot, I. B., Madhankumar, A., Umoren, S. A., &Gasem, Z. M. (2015). Surface protection of mild steel using benzimidazole derivatives: Experimental and theoretical approach. Journal of Adhesion Science and Technology, 29(19), 2130–2152.
11. Rbaa, M., Galai, M., Abousalem. A. S., Lakhrissi. B., Touhami. M. E., Warad. I., Zarrouk. (2019). Synthetic, spectroscopic characterization, empirical and theoretical investigations on the corrosion inhibition characteristics of mild steel in molar hydrochloric acid by three novel 8-hydroxyquinoline derivatives.Ionics, https://doi.org/10.1007/s11581-019-03160-9.
12. Singh, A., Ansari, K. R., Quraishi, M. A., Kaya, S. and Banerjee, P. The effect of anN-heterocyclic compound on corrosion inhibition of J55 steel in sweet corrosive medium, New Journal of Chemistry, 43 (2019) 6303-6313.
13. Yildiz, M., Gerengi, H., Solomon, M. M., Kaya, E., &Umoren, S. A. (2018). Influence of 1-butyl-1-methylpiperidinium tetrafluoroborate on St37 steel dissolution behavior in HCl environment. Chemical Engineering Communications, 205(4), 538–548.
14. Rani, B. E. A., &Basu, B. B. J. (2012). Green inhibitors for corrosion protection of metals and alloys: An overview. International Journal of Corrosion. https://doi.org/10.1155/2012/380217.
15. Lai, C., Guo, X., Wei, J., Xie, B., Zou, L., Li, X., … Wang, C. (2017). Investigation on Two Compounds of O,O’-dithiophosphate Derivatives as Corrosion Inhibitors for Q235 Steel in Hydrochloric Acid Solution. Open Chemistry, 15(1), 263–271.
16. Wang, J., Lin, Y., Singh, A., & Liu, W. (2018). Investigation of some porphyrin derivatives as inhibitors for corrosion of N80 steel at high temperature and high pressure in 3.5% NaCl solution containing carbon dioxide. International Journal of Electrochemical Science, 13(12), 11961–11973.
17. Qiang, Y., Zhang, S., Tan, B., & Chen, S. (2018). Evaluation of Ginkgo leaf extract as an eco-friendly corrosion inhibitor of X70 steel in HCl solution. Corrosion Science, 133, 6–16. Leena, P., ZeinulHukuman, N. H., Biju, A. R., &Jisha, M. (2019). Studies on methanolic extract of lepidagathiskeralensis as green corrosion

inhibitor for mild steel in 1M HCL. Journal of Electrochemical Science and Technology, 10(2), 231–243.

18. Singh, A., Ansari, K. R., Kumar, A., Liu, W., Songsong, C., & Lin, Y. (2017). Electrochemical, surface and quantum chemical studies of novel imidazole derivatives as corrosion inhibitors for J55 steel in sweet corrosive environment. Journal of Alloys and Compounds, 712, 121–133.
19. PreethiKumari, P., Shetty, P., & Rao, S. A. (2017). Electrochemical measurements for the corrosion inhibition of mild steel in 1 M hydrochloric acid by using an aromatic hydrazide derivative. Arabian Journal of Chemistry, 10(5), 653–663.
20. Reddy, A.S., Kumar, M.S., & Reddy, G.R., (2000). A convenient method for the preparation of hydroxamic acids, Tetrahedron Letters, 41, 6285–6288.
21. Farkas, E., Enyedy, E. A., Csoka, H., (1999). A comparison between the chelating properties of some dihydroxamic acids, desferrioxamine B and acetohydroxamic acid, Polyhedron, 18, 2391–2398.
22. Farkas, E., Enyedy, E.A., Zekany, L., &Deak, G., (2001). Interaction between iron (II) and hydroxamic acids: oxidation of iron (II) to iron (III) by desferrioxamine B under anaerobic conditions, Journal of Inorganic Biochemistry, 83, 107–114.
23. Alagta, A., Felhosi, I., &Kalman, E., (2007). Hydroxamic acid corrosion inhibitor for steel in aqueous solution, Material Science Forum, 537–538, 81–88.
24. Telegdi, J., Rigo, T., &Kalman. E., (2005). Molecular layers of hydroxamic acids in copper corrosion inhibition, Journal of Electroanalytical Chemistry, 582, 191–201.
25. Bahlakeh, G., Dehghani, A., Ramezanzadeh, B. And Ramezanzadeh, M. Highly effective mild steel corrosion inhibition in 1 M HCl solution by novel green aqueous Mustard seed extract: Experimental, electronic-scale DFT and atomic-scale MC/MD explorations, Journal of Molecular Liquids, 293 (2019)111559
26. Verma, D.K., Khan, F., (2016). Corrosion inhibition of mild steel in hydrochloric acid using extract of glycine max leaves, Research on Chemical Intermediates, 42, 3489–3506.
27. Singh, A., Ansari, K. R., Chauhan, D. S., Quraishi, M. A., Lgaz, H., & Chung, I. M. (2020). Comprehensive investigation of steel corrosion inhibition at macro/micro level by ecofriendly green corrosion inhibitor in 15% HCl medium. Journal of Colloid and Interface Science, 560, 225–236.

28. Verma, C., Quraishi, M. A., Ebenso, E. E., Obot, I. B., & El Assyry, A. (2016). 3-Amino alkylated indoles as corrosion inhibitors for mild steel in 1M HCl: Experimental and theoretical studies. Journal of Molecular Liquids, 219, 647–660.
29. Verma, D.K., Khan, F., I. Bahadur, I., Salman, M., Quraishi, M.A., Ebenso, E.E., & Verma, C., (2018). Inhibition performance of Glycine max, Cuscuta reflexa and Spirogyra extracts for mild steel dissolution in acidic medium: Density functional theory and experimental studies, Results in Physics, 10, 665–674.
30. Ahmed, M. H. O., Al-Amiery, A. A., Al-Majedy, Y. K., Kadhum, A. A. H., Mohamad, A. B., &Gaaz, T. S. (2018). Synthesis and characterization of a novel organic corrosion inhibitor for mild steel in 1 M hydrochloric acid. Results in Physics, 8, 728–733.
31. Verma, D.K., & Khan, F., (2016). Green approach to corrosion inhibition of mild steel in hydrochloric acid medium using extract of spirogyra algae, Green Chemistry Letters and Reviews, 9 (1), 52-60.
32. Singh, A., Ahamad, I., & Quraishi, M. A. (2016). Piper longum extract as green corrosion inhibitor for aluminium in NaOH solution. Arabian Journal of Chemistry, 9, S1584–S1589.
33. Fiori-Bimbi, M. V., Alvarez, P. E., Vaca, H., &Gervasi, C. A. (2015). Corrosion inhibition of mild steel in HCL solution by pectin. Corrosion Science, 92, 192–199.
34. Dutta, A., Saha, S. K., Adhikari, U., Banerjee, P., &Sukul, D. (2017). Effect of substitution on corrosion inhibition properties of 2-(substituted phenyl) benzimidazole derivatives on mild steel in 1 M HCl solution: A combined experimental and theoretical approach. Corrosion Science, 123, 256–266.
35. Singh, A., Ansari, K. R., Kumar, A., Liu, W., Songsong, C., & Lin, Y. (2017). Electrochemical, surface and quantum chemical studies of novel imidazole derivatives as corrosion inhibitors for J55 steel in sweet corrosive environment. Journal of Alloys and Compounds, 712, 121–133.
36. Yadav, M., Kumar, S., Tiwari, N., Bahadur, I., &Ebenso, E. E. (2015). Experimental and quantum chemical studies of synthesized triazine derivatives as an efficient corrosion inhibitor for N80 steel in acidic medium. Journal of Molecular Liquids, 212, 151–167.
37. Singh, A., Lin, Y., Ansari, K. R., Quraishi, M. A., Ebenso, E. E., Chen, S., & Liu, W. (2015). Electrochemical and surface studies of some Porphines as corrosion inhibitor

for J55 steel in sweet corrosion environment. Applied Surface Science, 359, 331–339.

38. Zhang, D., Tang, Y., Qi, S., Dong, D., Cang, H., & Lu, G. (2016). The inhibition performance of long-chain alkyl-substituted benzimidazole derivatives for corrosion of mild steel in HCl. Corrosion Science, 102, 517–522.
39. Abd El-Lateef, H. M., Abo-Riya, M. A., &Tantawy, A. H. (2016). Empirical and quantum chemical studies on the corrosion inhibition performance of some novel synthesized cationic gemini surfactants on carbon steel pipelines in acid pickling processes. Corrosion Science, 108, 94–110.
40. Abd El-Lateef, H. M., &Tantawy, A. H. (2016). Synthesis and evaluation of novel series of Schiff base cationic surfactants as corrosion inhibitors for carbon steel in acidic/chloride media: Experimental and theoretical investigations. RSC Advances, 6(11), 8681–8700.
41. Lgaz, H., Salghi, R., Jodeh, S., &Hammouti, B. (2017). Effect of clozapine on inhibition of mild steel corrosion in 1.0 M HCl medium. Journal of Molecular Liquids, 225, 271–280.
42. Hassannejad, H., &Nouri, A. (2018). Sunflower seed hull extract as a novel green corrosion inhibitor for mild steel in HCl solution. Journal of Molecular Liquids, 254, 377–382.
43. Alvarez, P. E., Fiori-Bimbi, M. V., Neske, A., Brandán, S. A., &Gervasi, C. A. (2018). Rolliniaoccidentalis extract as green corrosion inhibitor for carbon steel in HCl solution. Journal of Industrial and Engineering Chemistry, 58, 92–99.
44. Bedair, M. A., El-Sabbah, M. M. B., Fouda, A. S., &Elaryian, H. M. (2017). Synthesis, electrochemical and quantum chemical studies of some prepared surfactants based on azodye and Schiff base as corrosion inhibitors for steel in acid medium. Corrosion Science, 128, 54–72.
45. Solomon, M. M., Gerengi, H., &Umoren, S. A. (2017). Carboxymethyl Cellulose/Silver Nanoparticles Composite: Synthesis, Characterization and Application as a Benign Corrosion Inhibitor for St37 Steel in 15% H_2SO_4 Medium. ACS Applied Materials and Interfaces, 9(7), 6376–6389.
46. Chugh, B., Singh,A. K., Thakur, S., Pani, B., Lgaz, H., Chung, I. M., Jha, R., and Ebenso, E. E. (2020). Comparative investigation of corrosion-mitigating behaviour of thiadiazole-derived bis-schiff bases for mild steel in acid medium: experimental,

theoretical, and surface study. ACS Omega, https://dx.doi.org/10.1021/acsomega.9b04274.

47. Obot, I. B., Madhankumar, A., Umoren, S. A., &Gasem, Z. M. (2015). Surface protection of mild steel using benzimidazole derivatives: Experimental and theoretical approach. Journal of Adhesion Science and Technology, 29(19), 2130–2152.
48. Gaussian 09, Revision A.02, Frisch MJ, Trucks GW, Schlegel HB, Scuseria GE, Robb MA, Cheeseman JR, et al. Gaussian, Inc., Wallingford CT; 2009.
49. El Aoufir, Y., Lgaz, H., Bourazmi, H., Kerroum, Y., Ramli, Y., Guenbour, A., &Oudda, H. (2016). Quinoxaline derivatives as corrosion inhibitors of carbon steel in hydrochloridric acid media: Electrochemical, DFT and montecarlo simulations studies. Journal of Materials and Environmental Science, 7(12), 4330–4347.
50. Hadisaputra, S., Purwoko, A. A., Ilhamsyah, I., Hamdiani, S., Suhendra, D., Nuryono, N., &Bundjali, B. (2018). A combined experimental and theoretical study of (E)-ethyl 3-(4-methoxyphenyl)acrylate as corrosion inhibitor of iron in 1 M HCL solutions. International Journal of Corrosion and Scale Inhibition, 7(4), 633–647.
51. Khalaf, M. M., Tantawy, A. H., Soliman, K. A., &Abd El-Lateef, H. M. (2020). Cationic gemini-surfactants based on waste cooking oil as new ‘green’ inhibitors for N80-steel corrosion in sulphuric acid: A combined empirical and theoretical approaches. Journal of Molecular Structure, 1203.
52. Dehghani, A., Bahlakeh, G., Ramezanzadeh, B., &Ramezanzadeh, M. (2019). Potential of Borage flower aqueous extract as an environmentally sustainable corrosion inhibitor for acid corrosion of mild steel: Electrochemical and theoretical studies. Journal of Molecular Liquids, 277, 895–911.
53. Salarvand, Z., Amirnasr, M., Talebian, M., Raeissi, K., &Meghdadi, S. (2017). Enhanced corrosion resistance of mild steel in 1 M HCl solution by trace amount of 2-phenyl-benzothiazole derivatives: Experimental, quantum chemical calculations and molecular dynamics (MD) simulation studies. Corrosion Science, 114, 133–145.
54. Pournazari, S.,Moayed, M. H., & Rahimizadeh, M. (2013) Pages 20-31, In situ inhibitor synthesis from admixture of benzaldehyde and benzene-1,2-diamine along with $FeCl_3$ catalyst as a new corrosion inhibitor for mild steel in 0.5 M sulphuric acid. Corrosion Science, 71, 20-31.
55. Abd El-Lateef, H. M., Soliman, K. A., &Tantawy, A. H. (2017). Novel synthesized Schiff Base-based cationic gemini surfactants: Electrochemical investigation,

theoretical modeling and applicability as biodegradable inhibitors for mild steel against acidic corrosion. Journal of Molecular Liquids, 232, 478–498.

56. Khalaf, M. M., Tantawy, A. H., Soliman, K. A., & Abd El-Lateef, H. M. (2020). Cationic gemini-surfactants based on waste cooking oil as new ‘green’ inhibitors for N80-steel corrosion in sulphuric acid: A combined empirical and theoretical approaches. Journal of Molecular Structure, 1203. https://doi.org/10.1016/j.molstruc.2019.127442.

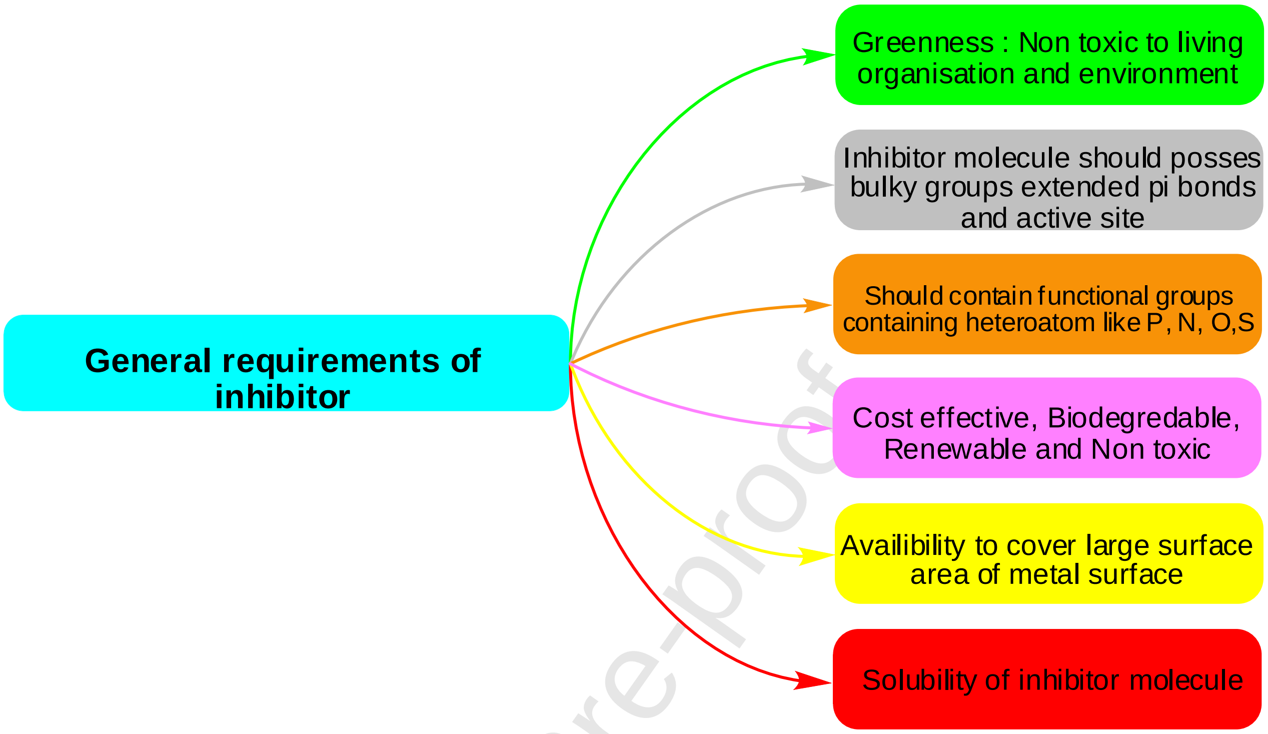

Figure 1: Schematic illustrations of basic requirrements of corrosion inhibitors.

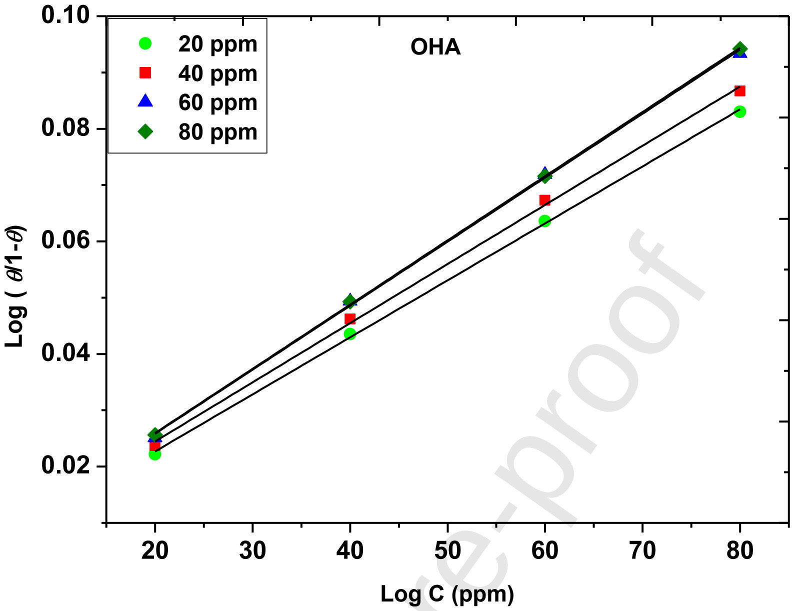
0.10
0.08
0.06
0.04
0.02
Log (θ/1-θ)
20
30
40
50
60
70
80
Log C (ppm)
OHA
20 ppm
40 ppm
60 ppm
80 ppm

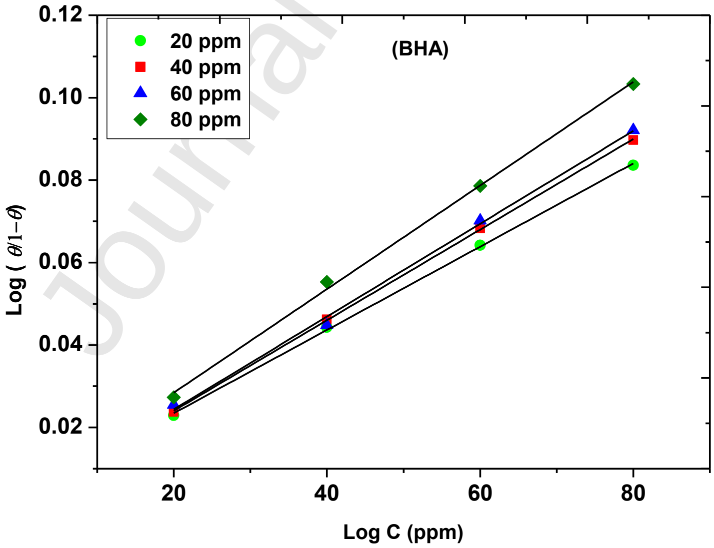
0.12
0.10
0.08
0.06
0.04
0.02
Log (θ/1−θ)
20
40
60
80
Log C (ppm)
(BHA)
20 ppm
40 ppm
60 ppm
80 ppm

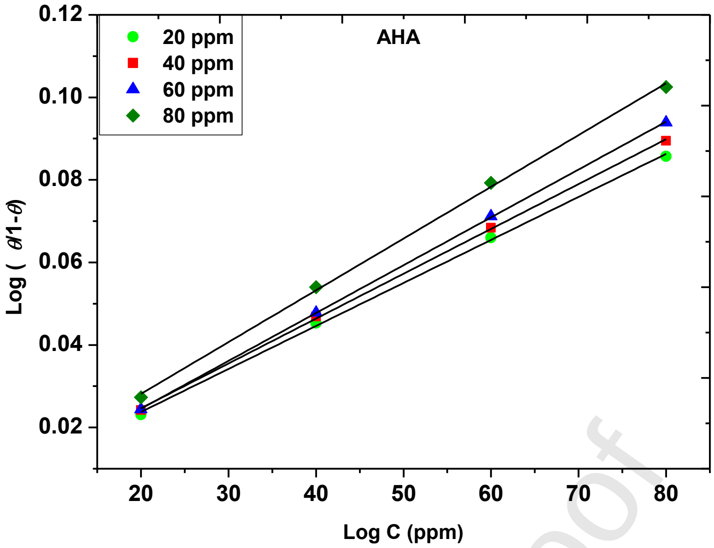

Figure 2: Langmuir plots of Log C (ppm) vs Log (θ/1-θ) for adsorption of OHA, BHA and AHA molecules on MS surface in 1M HCl.

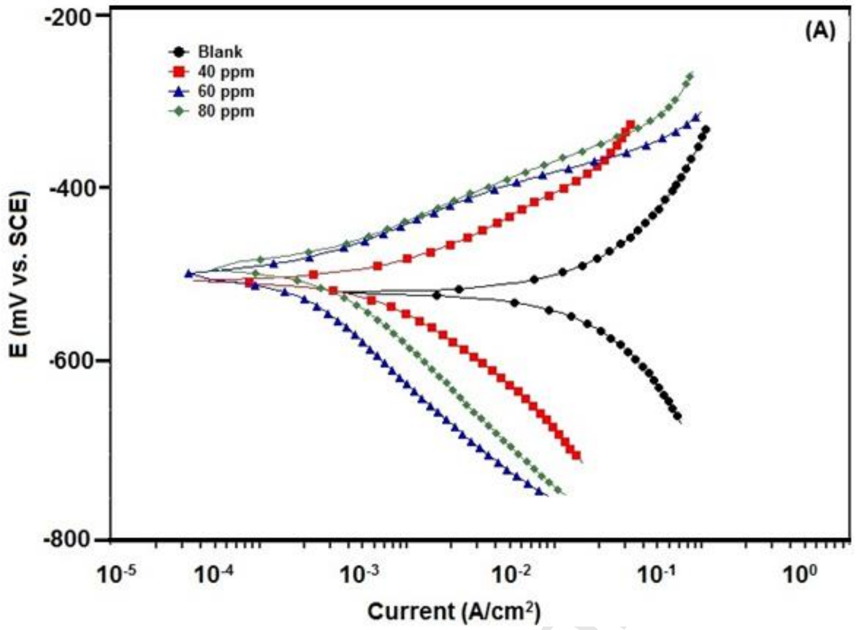
(A)
Blank
40 ppm
60 ppm
80 ppm
E (mV vs. SCE)
-200
-400
-600
-800
10-5
10-4
10-3
10-2
10-1
100
Current (A/cm2)

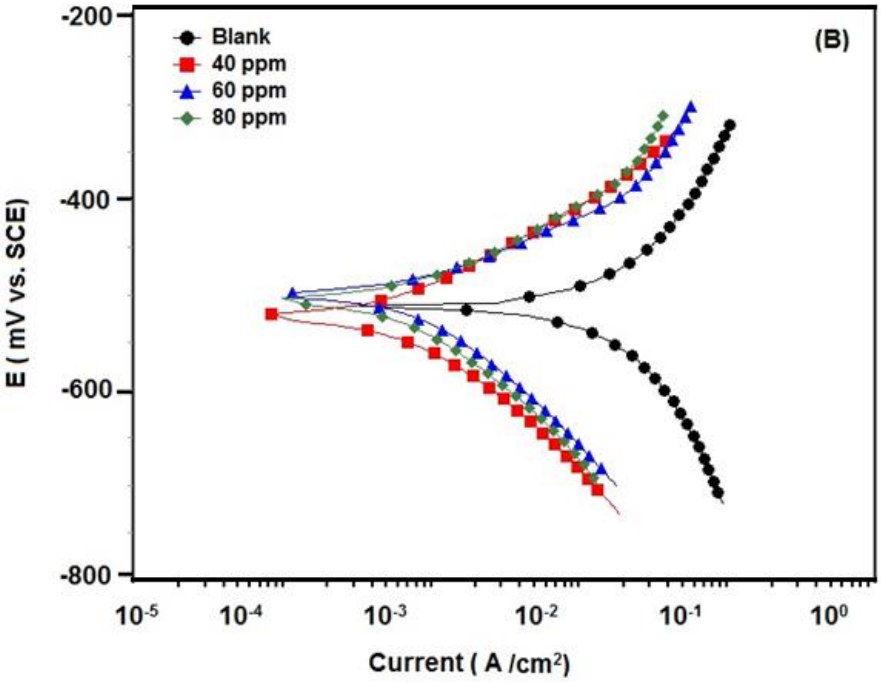
(B)
Blank
40 ppm
60 ppm
80 ppm
E (mV vs. SCE)
-200
-400
-600
-800
10-5
10-4
10-3
10-2
10-1
100
Current (A /cm2)

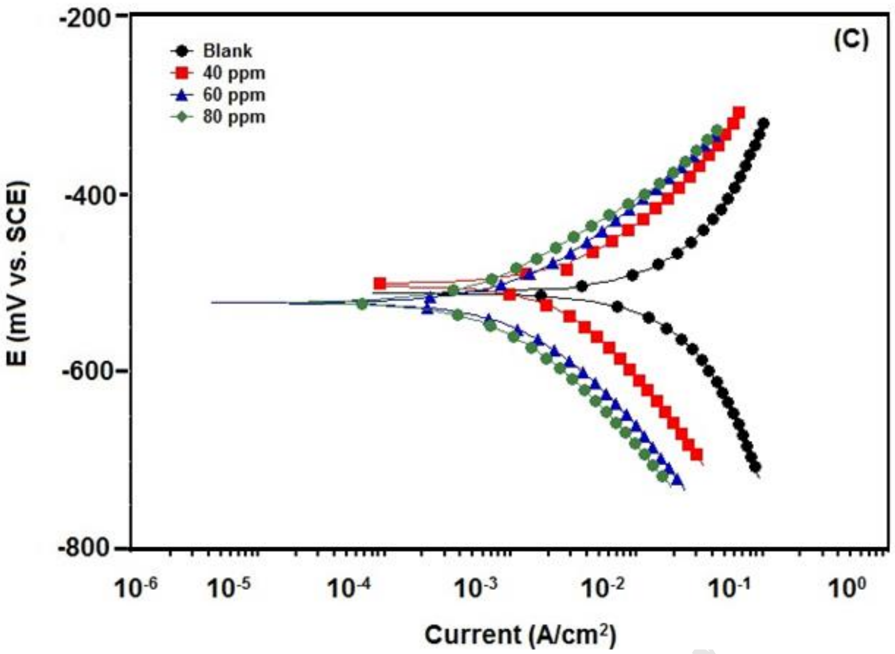

Figure 3: Potentiodynamic polarization curves for mild steel in molar concentration of hydrochloric acid (1 M HCl) and different concentrations (40-80 ppm) of (a) OHA, (b) BHA and (c) AHA at room temperature.

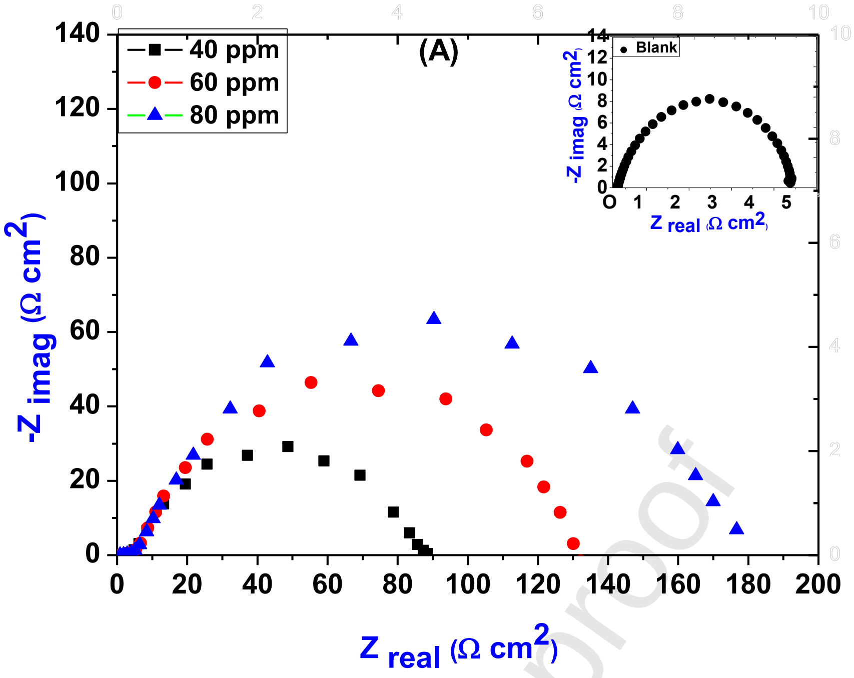
(A)
40 ppm
60 ppm
80 ppm
-Z imag (Ω cm^2)
Z real (Ω cm^2)
0
20
40
60
80
100
120
140
160
180
200
Blank
-Z imag (Ω cm2)
Z real Ω cm2
0
2
4
6
8
10
12
14
1
2
3
4
5

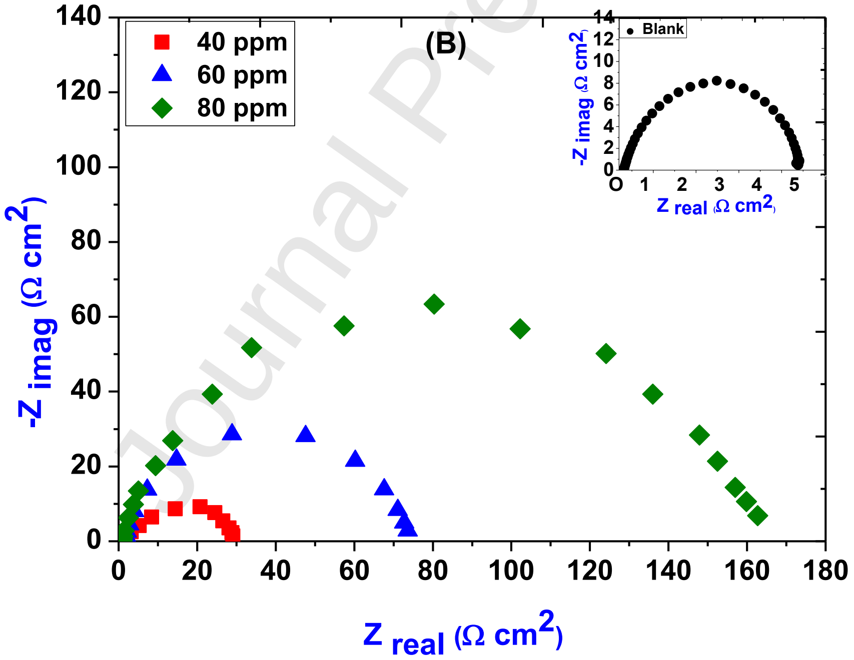
(B)
40 ppm
60 ppm
80 ppm
-Z imag (Ω cm^2)
Z real (Ω cm^2)
0
20
40
60
80
100
120
140
160
180
Blank
-Z imag (Ω cm2)
Z real Ω cm2
0
2
4
6
8
10
12
14
1
2
3
4
5

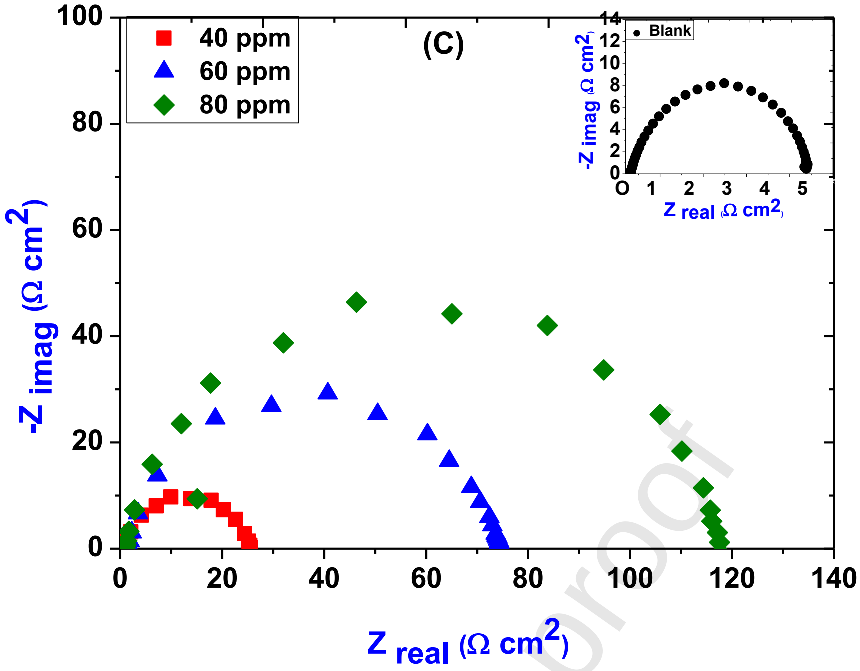

Figure 4: Nyquist plots for mild steel in molar concentration of hydrochloric acid (1 M HCl) and different concentrations (40-80 ppm) of (a) OHA, (b) BHA and (c) AHA at room temperature.

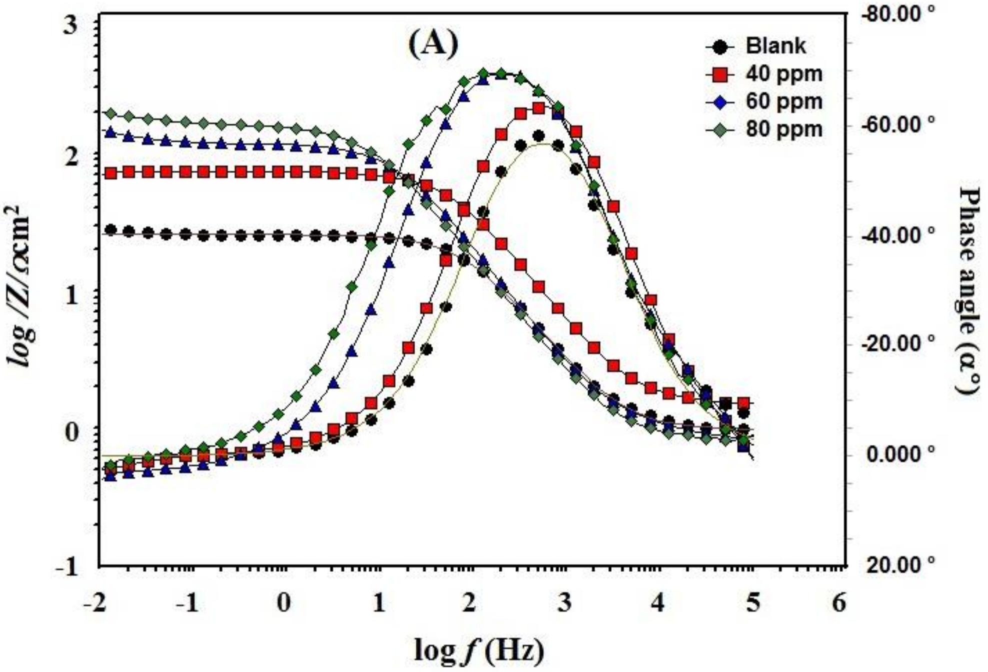
(A)
Blank
40 ppm
60 ppm
80 ppm
log /Z/ Ωcm^2
Phase angle (α°)
log f (Hz)
3
2
1
0
-1
-80.00 °
-60.00 °
-40.00 °
-20.00 °
0.000 °
20.00 °
-2
-1
0
1
2
3
4
5
6

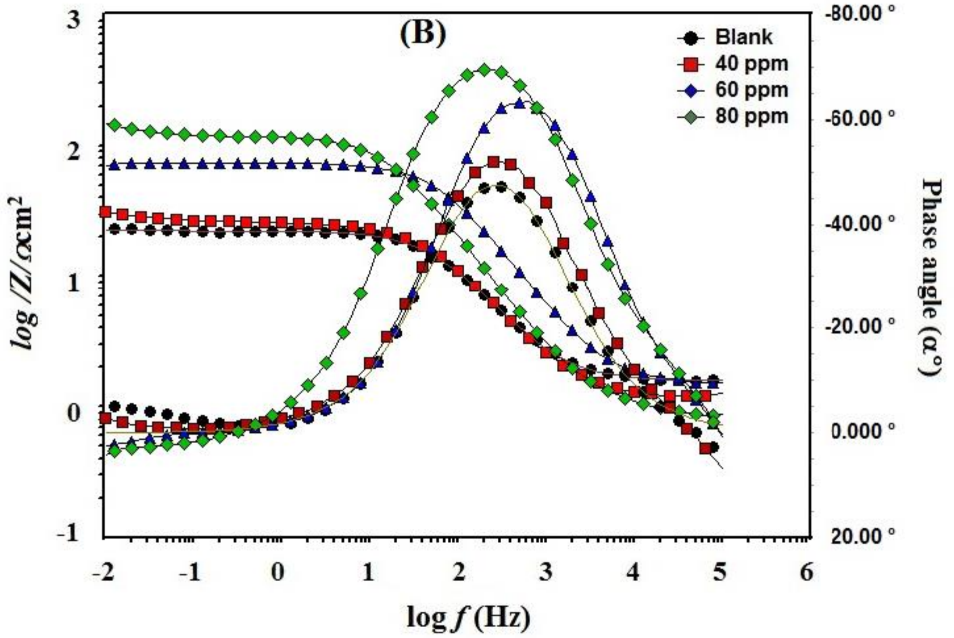
(B)
Blank
40 ppm
60 ppm
80 ppm
log /Z/ Ωcm^2
Phase angle (α°)
log f (Hz)
3
2
1
0
-1
-80.00 °
-60.00 °
-40.00 °
-20.00 °
0.000 °
20.00 °
-2
-1
0
1
2
3
4
5
6

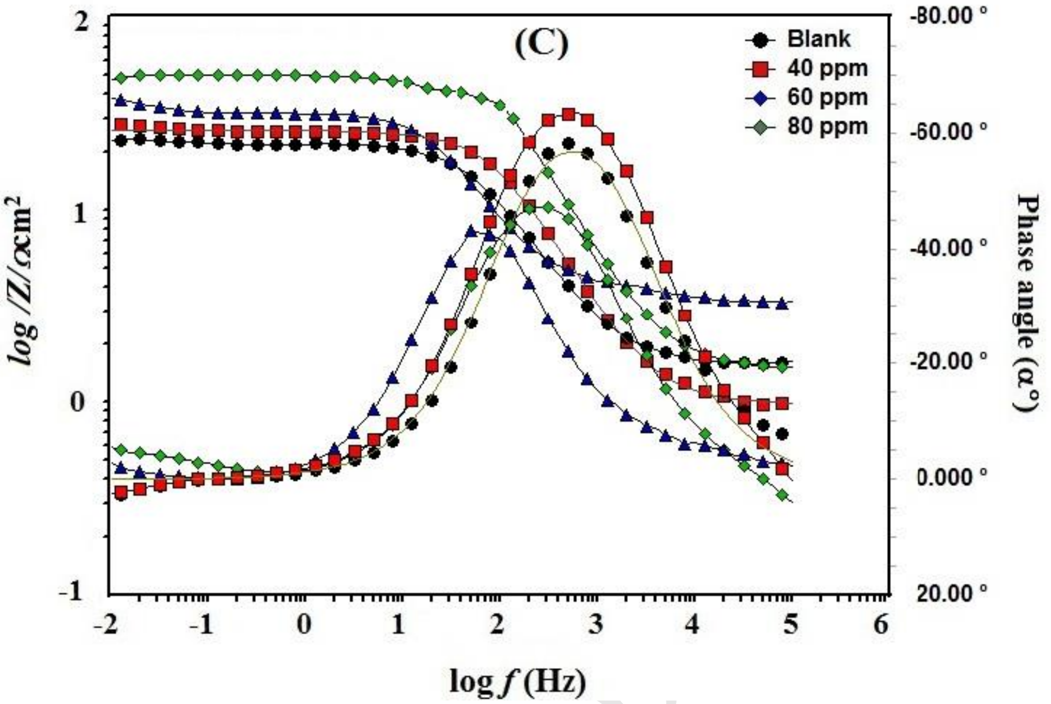

Figure 5: Bode (log *f* vs log |Z| & phase angle (log *f* vs –phase) plots for mild steel in 1 M HCl and different concentrations (40-80 ppm) of (a) OHA, (b) BHA and (c) AHA at room temperature

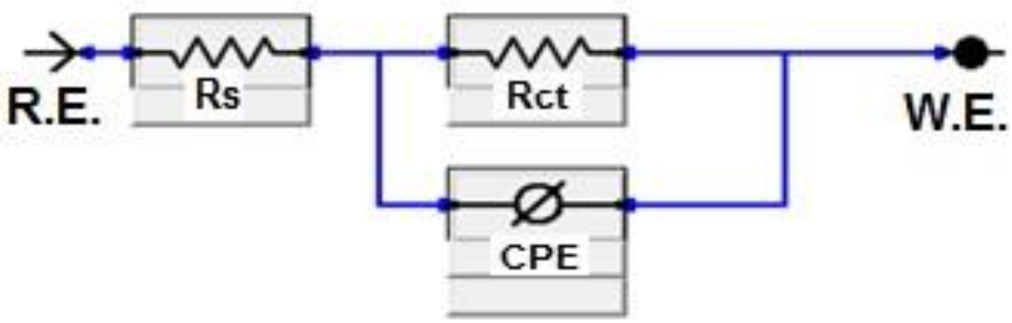

Figure 6: Equivalent circuit model applied for fitting of the impedance spectra

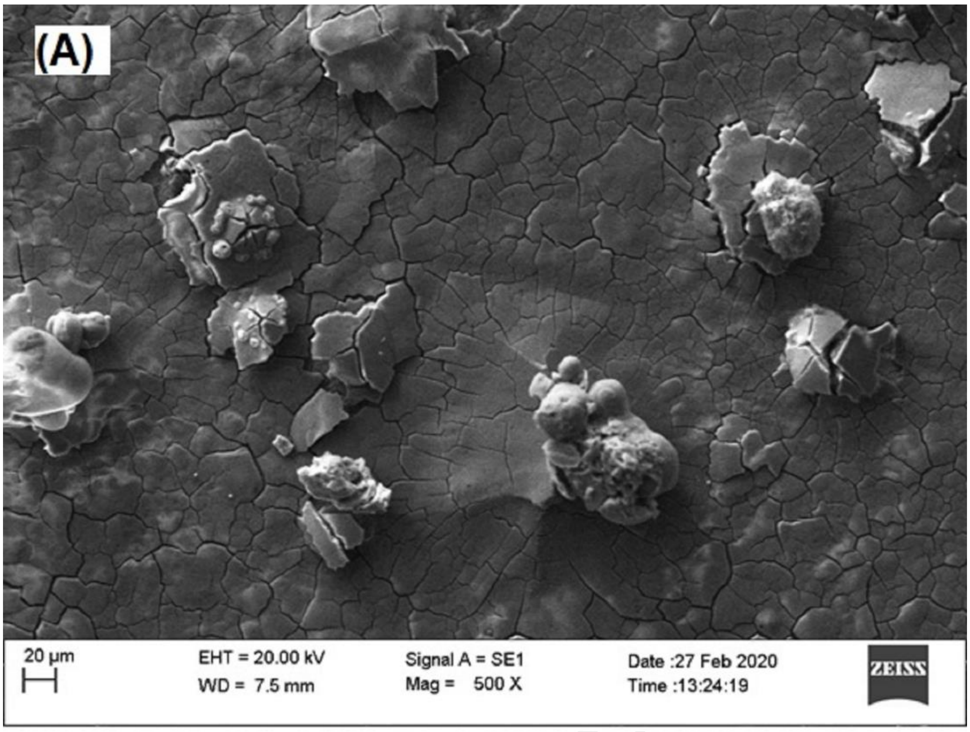
(A)
20 µm
EHT = 20.00 kV
WD = 7.5 mm
Signal A = SE1
Mag = 500 X
Date :27 Feb 2020
Time :13:24:19
ZEISS

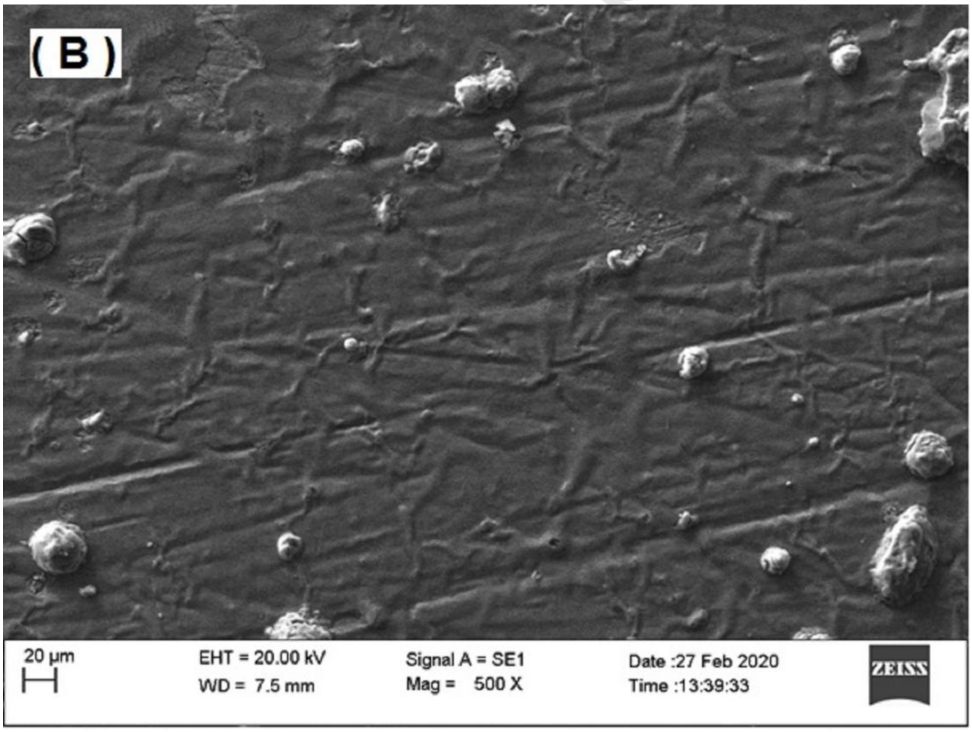
(B)
20 µm
EHT = 20.00 kV
WD = 7.5 mm
Signal A = SE1
Mag = 500 X
Date :27 Feb 2020
Time :13:39:33
ZEISS

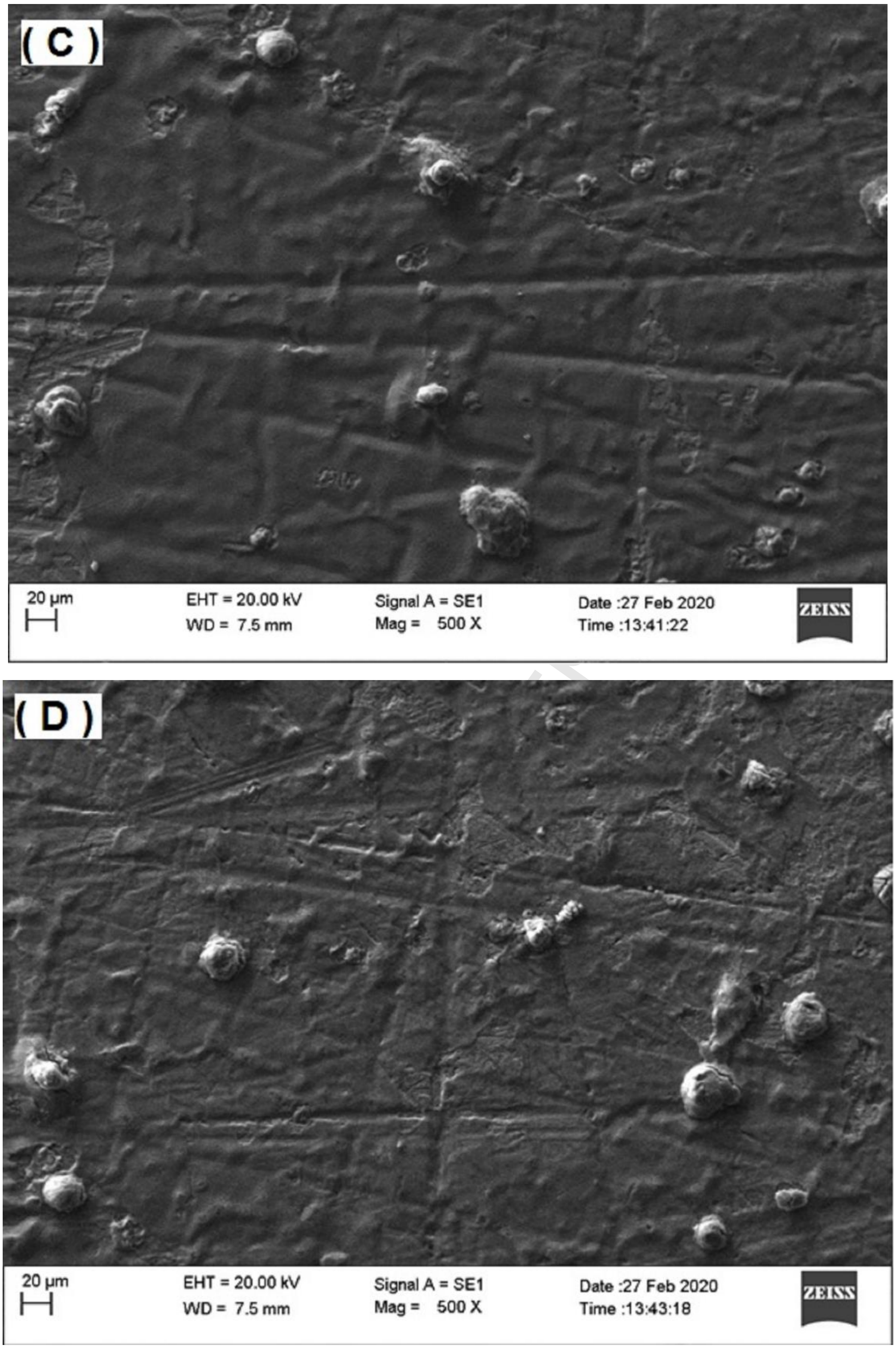

Figure 7:SEM microphotographs of mild steel in molar concentration of hydrochloric acid (1 M HCl) after 6h immersion period at 298 K (a) after immersion in 1 M HCl, (b) after immersion with 80 ppm OHA, (c) after immersion with 80 ppm BHA and (d) after immersion with 80 ppm AHA

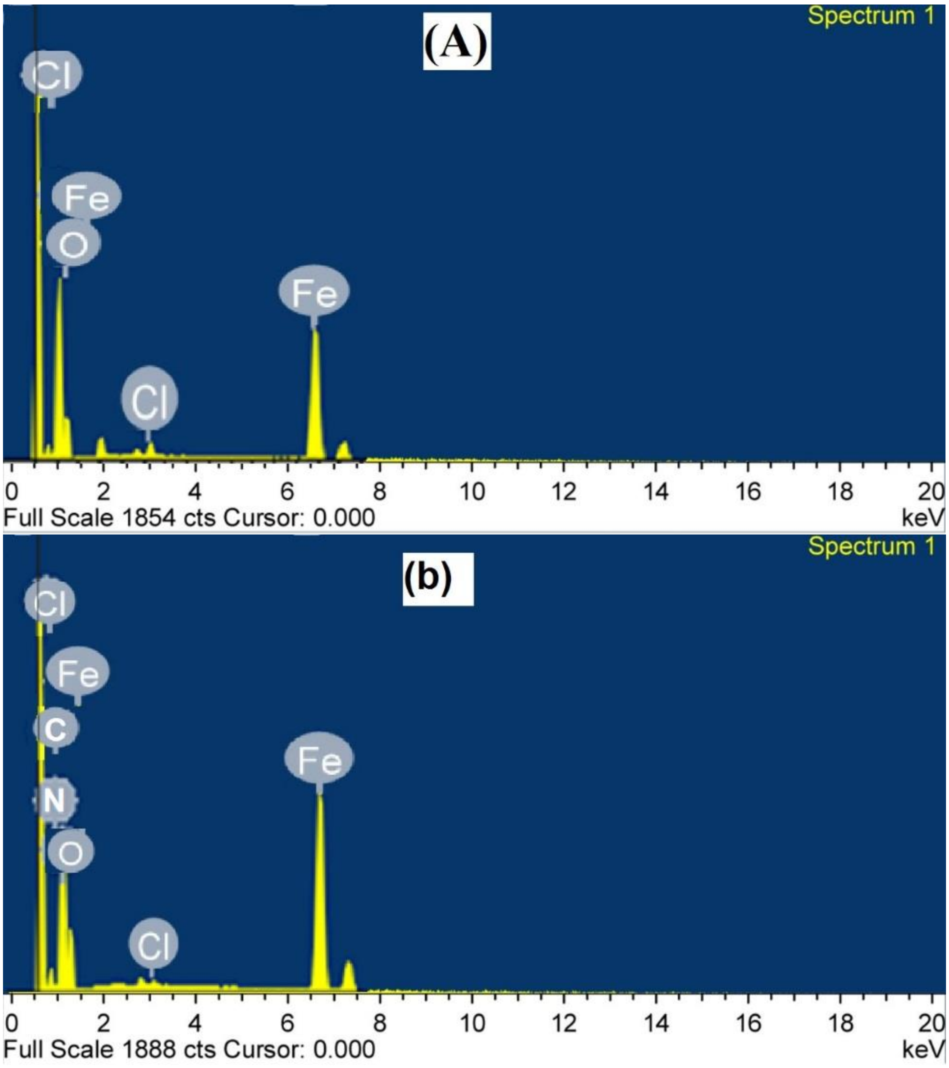
(A)
Spectrum 1
Cl
Fe
O
Fe
Cl
0
2
4
6
8
10
12
14
16
18
20
Full Scale 1854 cts Cursor: 0.000
keV
(b)
Spectrum 1
Cl
Fe
C
N
O
Fe
Cl
0
2
4
6
8
10
12
14
16
18
20
Full Scale 1888 cts Cursor: 0.000
keV

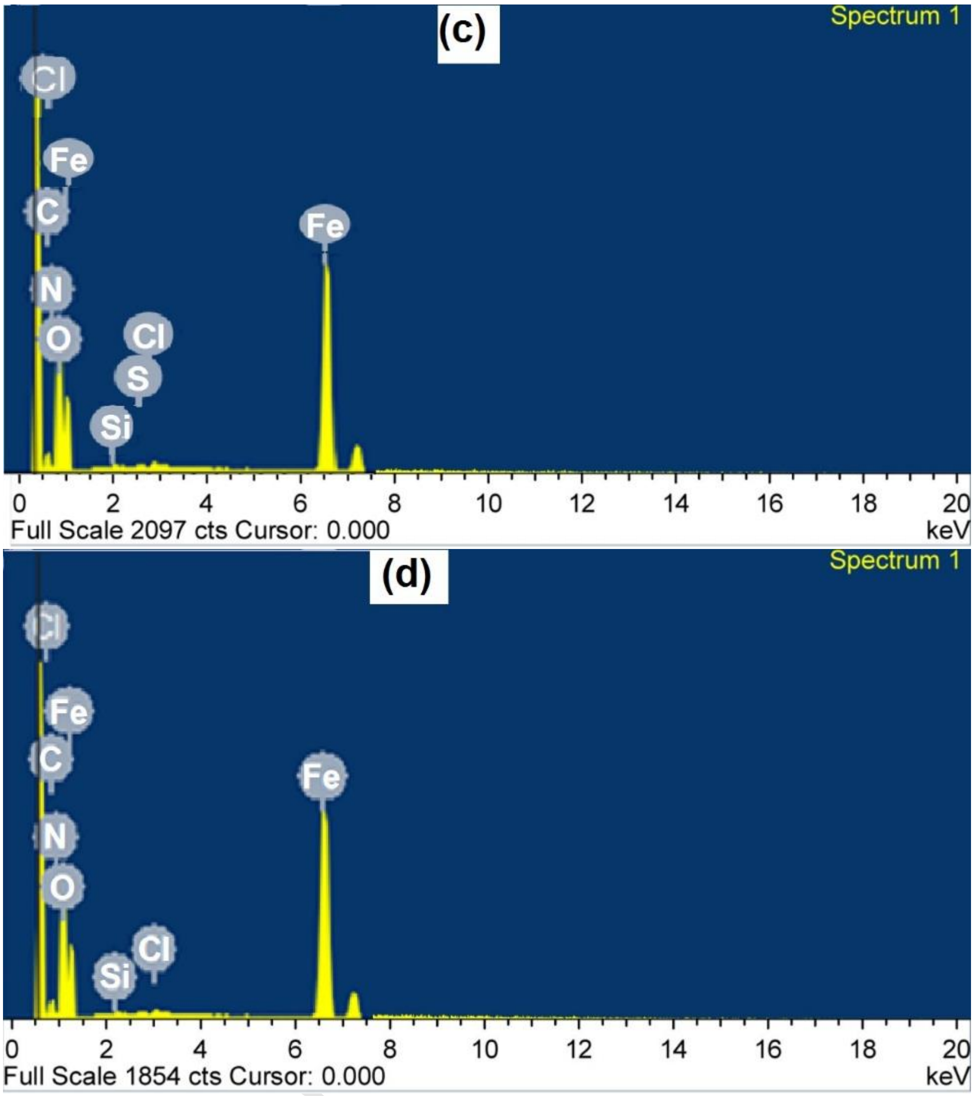

Figure 8:EDS spectra of mild steel coupons in molar concentration of hydrochloric acid (1 M HCl) (a) after immersion in 1 M HCl, (b) after immersion with 80 ppm OHA, (c) after immersion with 80 ppm BHA and (d) after immersion with 80 ppm AHA.

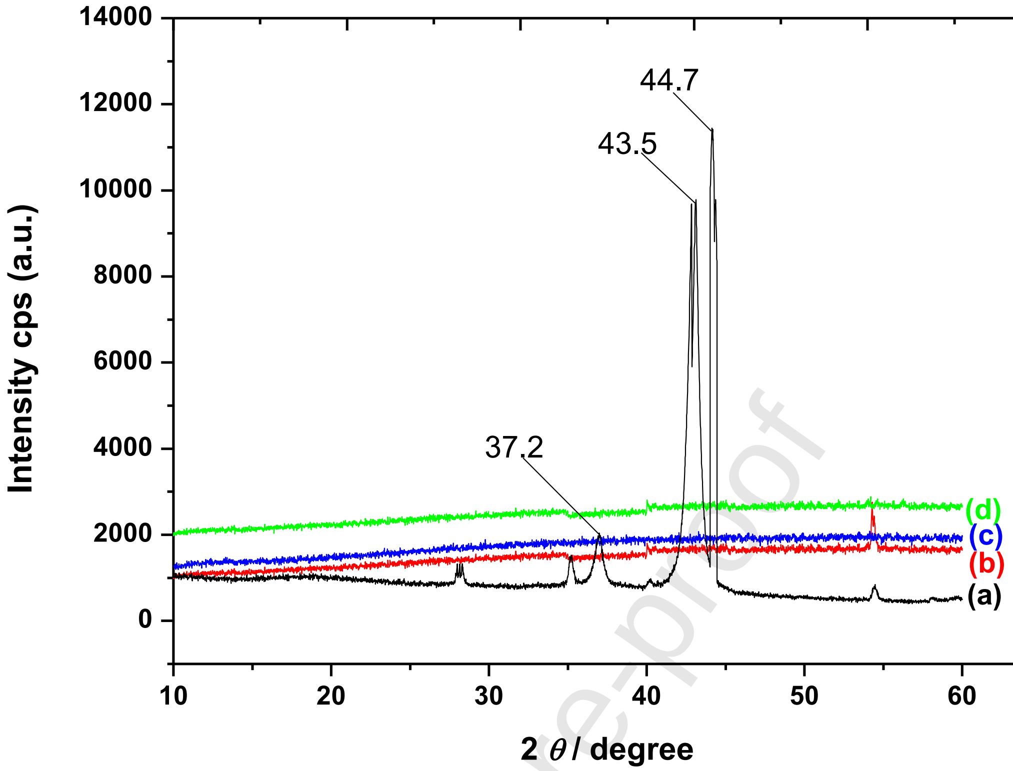

Fig. 9. XRD pattern of scratches sample of mild steel in 1 M HCl (a) after immersion in 1 M HCl, (b) after immersion with 80 ppm OHA, (c) after immersion with 80 ppm BHA and (d) after immersion with 80 ppm AHA.

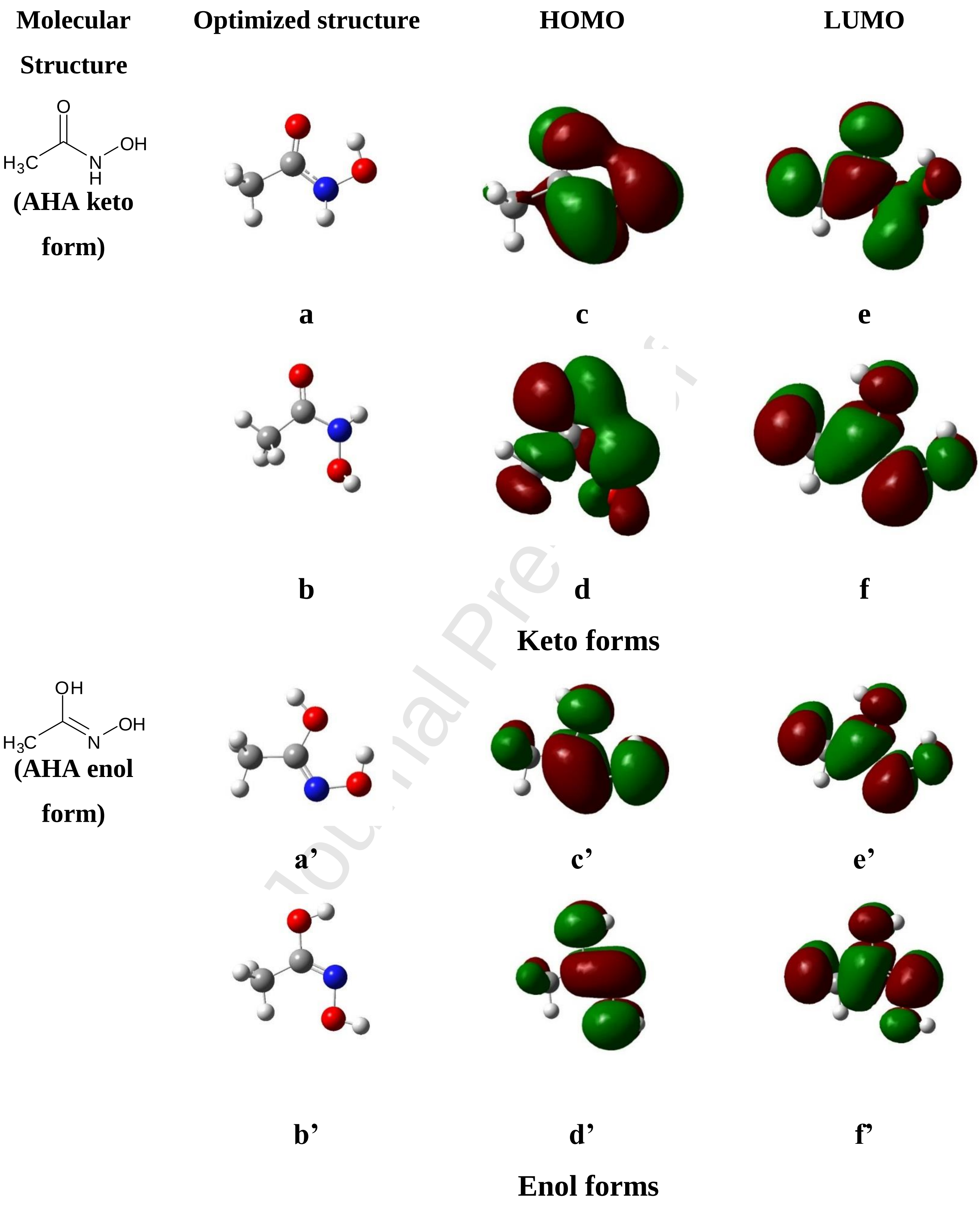

Fig. 10. The optimized structure (left), HOMO (middle) and LUMO (right) for keto and enol forms of AHA respectively.

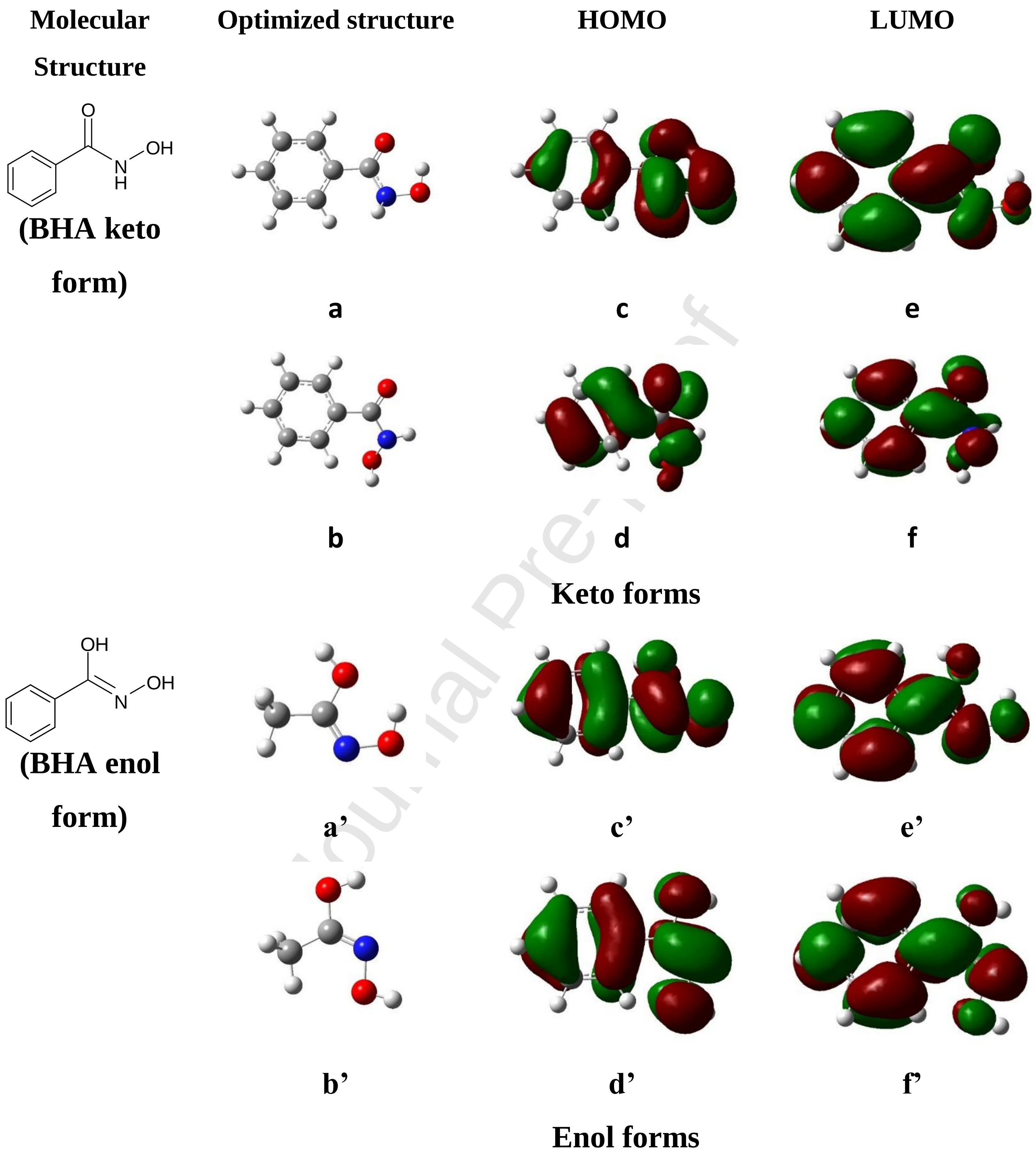

Fig. 11. The optimized structure (left), HOMO (middle) and LUMO (right) for keto and enol forms of AHA respectively.

Molecular Structure **Optimized structure** **HOMO** **LUMO**

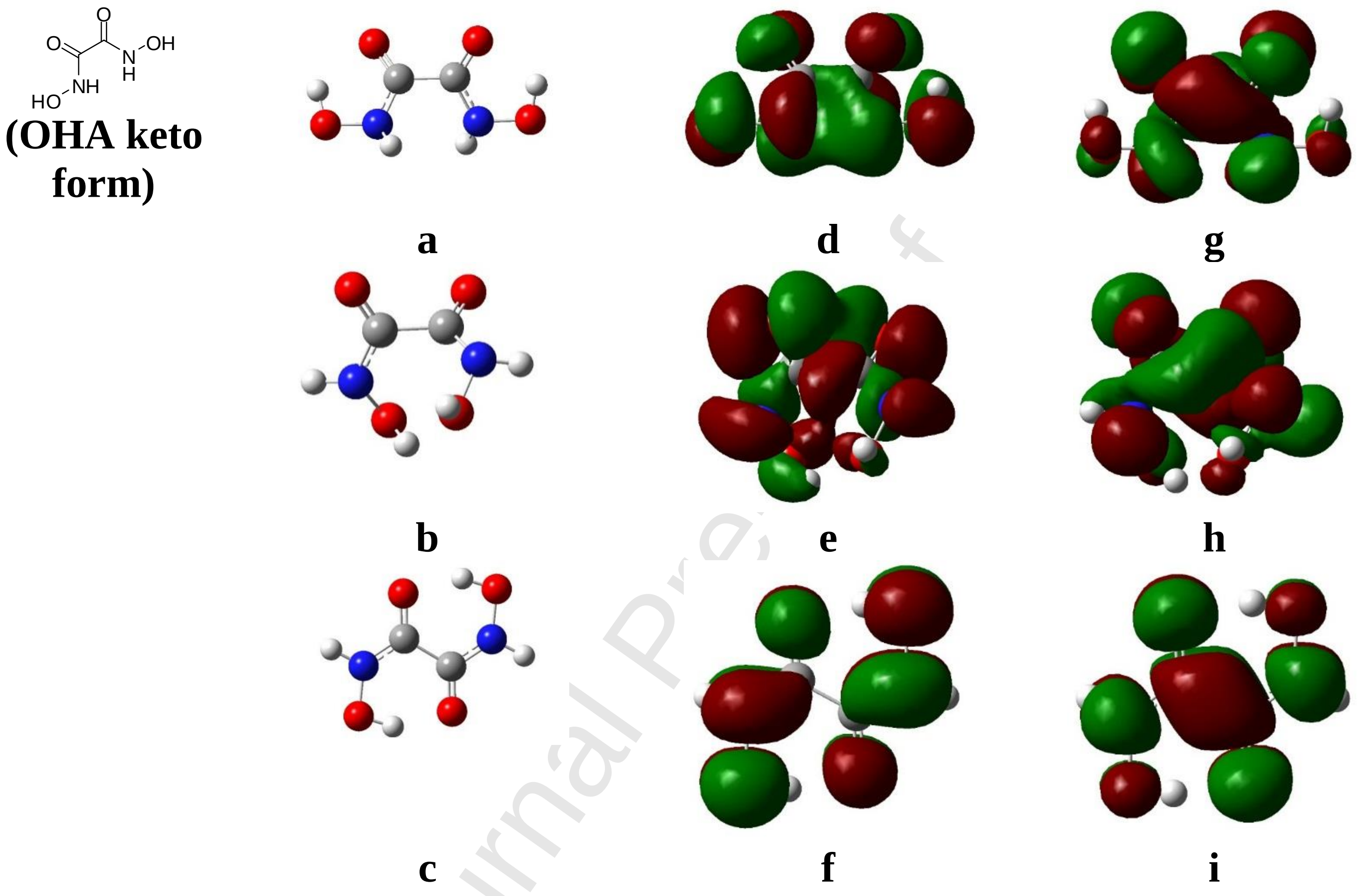

Keto forms

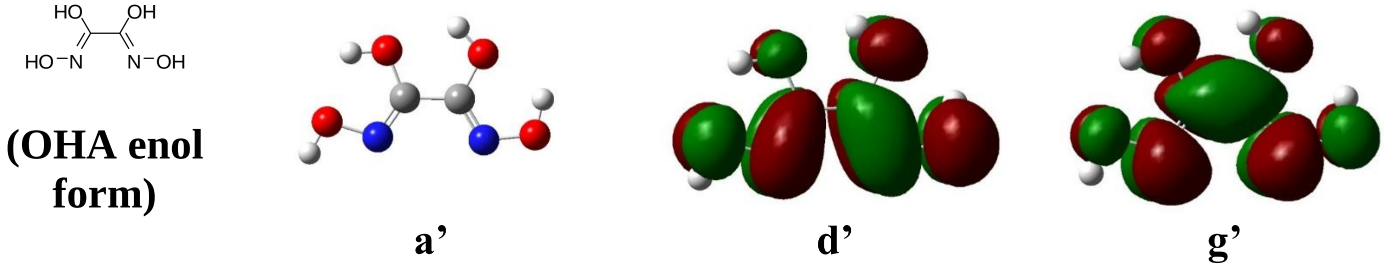

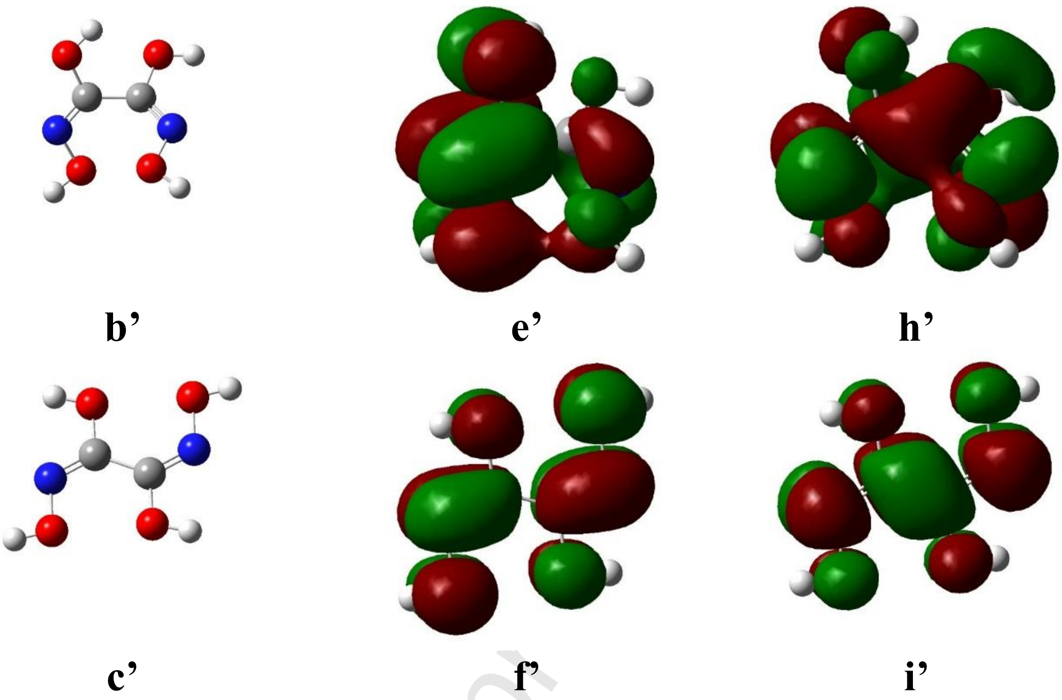

Enol forms

Fig. 12. The optimized structure (left), HOMO (middle) and LUMO (right) for keto and enol forms of AHA respectively.

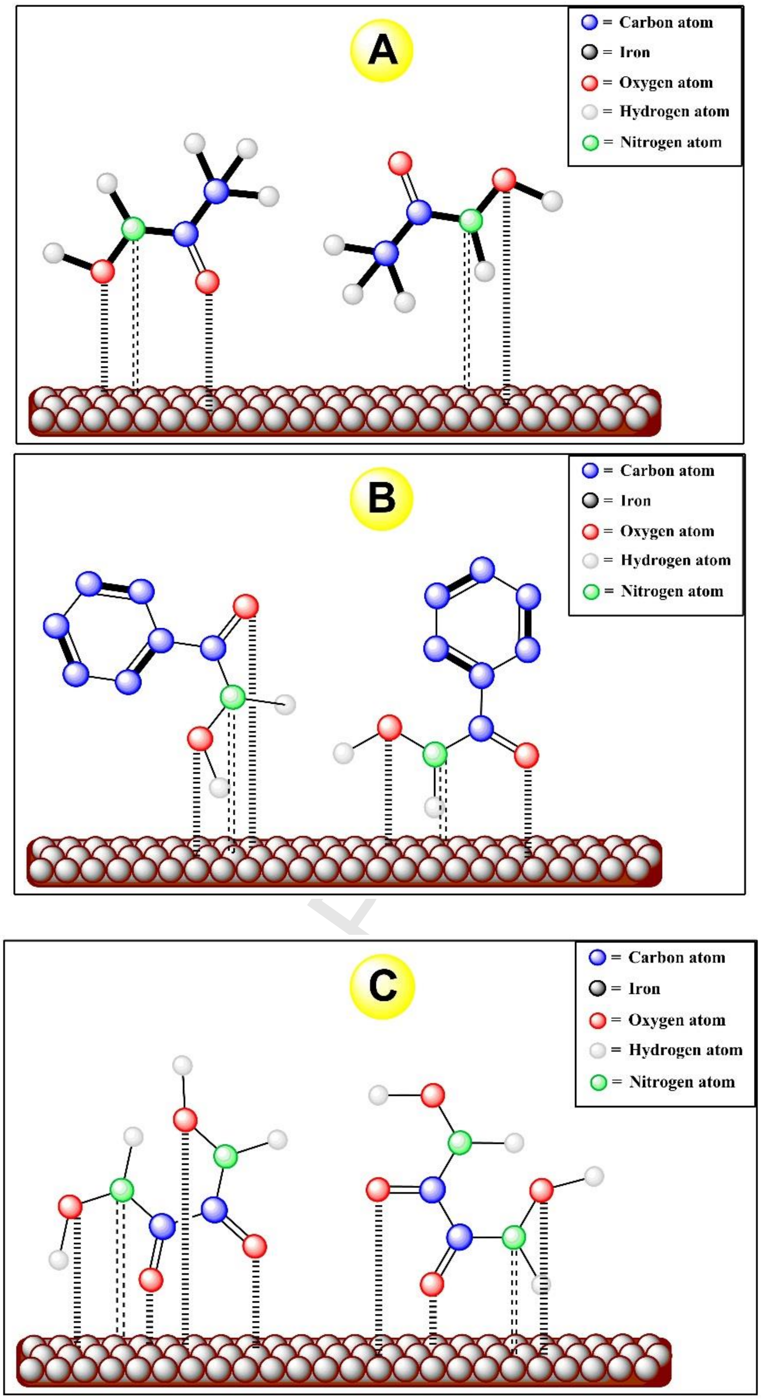

Fig. 13: Possible adsorption mechanism of a) AHA b) BHA and, c) OHA onto metal surface in 1 M HCl aqueous solution.

Table 1: IUPAC names, Chemical structures, abbreviations and analytical data of the investigated inhibitor (AHA, BHA and OHA) molecules.

S. No.	IUPAC name	Structures	Analytical and spectral data
1	***N*-hydroxyacetamide** (Acetohydroxamic acid) AHA	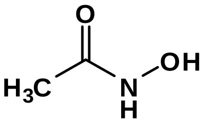	$C_2H_5NO_2$; Mol. wt.:75.07D; M. P.: 88°C±1, IR (KBr): 3227.85, 2868.93, 1659.64, 1449.79, 1376.02; ^{1}HNMR (DMSO, δ, ppm): 8.72, 2.1, 2.2; ^{13}CNMR (DMSO, δ, ppm): 173.9, 38.8
2	***N*-hydroxybenzamide** (Benzohydroxamic acid) BHA	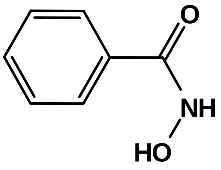	$C_7H_7NO_2$; Mol. wt.:231.20D; M. P.: 128°C ±1, IR (KBr): 3298.05, 2754.55, 1646.72, 1636.44, 1315.86; ^{1}HNMR (DMSO, δ, ppm): 7.61, 7.8, 2.60; ^{13}CNMR (DMSO, δ, ppm): 164.6, 128.81, 39.94
3	***N^1*,*N^2*-dihydroxyoxalamide** (Oxalohydroxamic acid) OHA	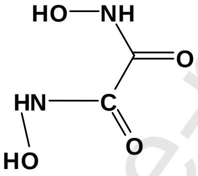	$C_2H_4N_2O_4$; Mol. wt.:120.06D; M. P.: 161°C ±1, IR (KBr):3271.87, 1654.81, 1442.14; ^{1}HNMR (DMSO, δ, ppm): 10.2, 2.5; ^{13}CNMR (DMSO, δ, ppm): 157.20

Table 2: Parameters derived from weight loss measurements in the absence and presence of inhibitors at different concentrations (20-80 ppm) and temperature (298 – 328 K) for mild steel in 1 M HCl.

Inhibitor	**Conc. (ppm)**	**Corrosion Rate, *ρ*, (mg cm^{-2} h^{-1})**				**Inhibition Efficiency (%*IE*)**			
		298K	**308K**	**318K**	**328K**	**298K**	**308K**	**318K**	**328K**
OHA	Blank	0.854	1.562	3.088	4.665	-	-	-	-
	20	0.085	0.245	0.631	1.021	90.04	84.31	79.57	78.11
	40	0.069	0.201	0.587	0.880	91.92	86.56	80.99	81.14
	60	0.049	0.168	0.513	0.755	94.26	89.24	83.39	83.82
	80	0.031	0.122	0.445	0.704	**96.37**	92.19	85.59	84.91
BHA	Blank	0.766	1.585	3.447	4.878	-	-	-	-
	20	0.098	0.255	0.744	1.302	87.20	83.91	78.41	73.31
	40	0.075	0.214	0.589	1.213	90.20	86.49	82.91	75.13
	60	0.050	0.198	0.502	1.156	93.47	87.50	85.44	76.30
	80	0.033	0.172	0.455	1.103	**95.69**	89.14	86.80	77.39
AHA	Blank	0.954	1.445	3.144	4.551	-	-	-	-
	20	0.131	0.252	0.568	1.222	86.26	82.56	81.93	73.15
	40	0.112	0.213	0.514	1.178	88.26	85.26	83.65	74.12
	60	0.087	0.178	0.495	1.104	90.88	87.68	84.25	75.74
	80	0.064	0.153	0.466	0.998	**93.29**	89.41	85.18	78.07

Table 3: Gibb's free energies (ΔG_{ads}) and adsorption constants (K_{ads}) values without and with inhibitors at different concentration (20-80 ppm) and temperature (298 – 328 K) for mild steel in 1 M HCl.

Inhibitor	**Temp. (K)**	R^2	K_{ads} (L mol^{-1})	ΔG_{ads} (kJ mol^{-1})
OHA	-	-	-	-
	298	0.9993	416.66	-24.890
	308	0.9983	294.12	-24.833
	318	0.9988	322.58	-25.882
	328	0.9978	322.58	-26.705
BHA	-	-	-	-
	298	0.9992	312.50	-24.177
	308	0.9980	500.00	-26.198
	318	0.9969	555.50	-27.318
	328	0.9978	303.03	-26.524
AHA	-	-	-	-
	298	0.9989	344.83	-24.422
	308	0.9995	344.83	-25.240
	318	0.9999	322.58	-25.882
	328	0.9985	333.33	-26.794

Table 4: Parameters derived from Tafel polarisation in the absence and presence of inhibitors at different concentration (20-80 ppm) and temperature (298 – 328 K) for mild steel in 1 M HCl.

Inhibitors	**Concentration**	**Tafel polarisation parameters**

	(ppm)	I_{corr} ($\mu A/cm^2$)	E_{corr} (mV vs SCE)	β_a (mV dec^{-1})	β_c (mV dec^{-1})	$\%\eta_{(PDP)}$	$\%IE_{(WL)}$
	Blank	86.31	-518	270.9	305.5	-	-
OHA	**40**	8.707	-507	85.22	142.6	89.91	91.92
	60	6.285	-500	77.60	188.2	92.71	94.26
	80	4.557	-491	82.67	161.3	**94.72**	**96.37**
BHA	**40**	11.13	-522	58.81	58.33	87.10	90.20
	60	08.86	-504	75.24	128.5	89.73	93.47
	80	05.18	-507	84.41	140.4	**93.99**	**95.69**
AHA	**40**	12.25	-510	110.4	192.0	85.80	88.26
	60	09.36	-504	124.4	222.1	89.15	90.88
	80	07.58	-518	107.1	131.3	**91.21**	**93.29**

Table 5: Parameters derived from electrochemical impedance spectroscopy (EIS) in the absence and presence of inhibitors at different concentration (20-80 ppm) and temperature (298 – 328 K) for mild steel in 1 M HCl.

Inhibitor	**Conc. (ppm)**	R_s (Ω)	R_{ct} (Ω cm^2)	C_{dl} (μF cm^{-2})	$\%\eta_{EIS}$	$\%IE_{WL}$
	Blank	0.985	05.22	122.4	-	-
OHA	**40**	1.522	88.40	83.51	94.09	91.92
	60	0.906	131.2	80.23	96.02	94.26
	80	0.844	181.7	69.95	**97.12**	**96.37**
BHA	**40**	1.022	29.83	107.8	82.50	90.20
	60	1.561	73.48	87.45	92.89	93.47
	80	2.314	166.2	63.02	**96.85**	**95.69**
AHA	**40**	1.554	25.22	74.01	79.30	88.26
	60	1.582	74.09	52.23	92.95	90.88
	80	3.498	119.6	31.14	**95.63**	**93.29**

Table 6: Percentage composition (wt %) of elements of mild steel surface in the absence and presence of inhibitors (80 ppm each) obtained from EDS spectral method.

Media	Composition (wt %)							
	Fe	**Cl**	**O**	**C**	**S**	**N**	**P**	**Cr**
Mild Steel (MS)	99.60	-	0.08	0.18	0.06	-	0.04	0.04
MS in 1 M HCl	92.92	5.88	1.20	-	-	-	-	-
MS in AHA + HCl solution	88.71	0.31	3.41	4.44	-	3.13	-	-
MS in BHA + HCl solution	87.15	0.40	3.30	5.04	-	4.11	-	-
MS in OHA + HCl solution	87.15	0.48	3.42	5.13	0.03	3.80	-	-

Table 7: DFT parameters derived for different tautomers and conformational isomers of AHA, BHA, OHA.

Compound	E_{HOMO} (eV)	E_{LUMO} (eV)	ΔE (eV)	IE	EA	η (eV)	χ (eV)	σ (eV)
AHA								

Keto-I	-6.50	0.18	6.68	6.50	-0.18	3.34	3.34	0.299
Keto-II	-6.90	0.20	7.10	6.90	-0.20	3.55	3.55	0.281
Enol-I	-6.27	0.78	7.05	6.27	-0.78	3.52	3.52	0.284
Enol-II	-6.14	0.80	6.94	6.14	-0.80	3.47	3.47	0.288
BHA								
Keto-I	-6.47	-1.36	5.11	6.47	1.36	2.55	3.91	0.392
Keto-II	-6.84	-1.22	5.62	6.84	1.22	2.87	4.03	0.348
Enol-I	-6.11	-1.07	5.04	6.11	1.07	2.52	3.59	0.396
Enol-II	-6.02	-0.92	5.10	6.02	0.92	2.55	3.24	0.392
OHA								
Keto-I	-7.18	-1.78	5.40	7.18	1.78	2.70	4.48	0.370
Keto-II	-6.93	-0.86	6.06	6.93	0.86	3.03	3.89	0.330
Keto-III	-6.75	-1.76	4.99	6.75	1.76	2.49	4.255	0.401
Enol-I	-6.26	-1.12	5.14	6.26	1.12	2.57	3.69	0.389
Enol-II	-6.30	-0.82	5.48	6.30	0.82	2.74	3.56	0.364
Enol-III	-6.01	-1.06	4.96	6.01	1.06	2.48	3.53	0.403

Highlights

1. Three hydroxamic acids (HAs) used as corrosion inhibitors for mild steel in 1M HCl.
2. Their effectiveness followed the sequence: OHA (96.37%) > BHA (95.69%) > AHA (93.29%).
3. HAs acted as mixed type corrosion inhibitors.
4. Adsorption of HAs on metal-1M HCl interfaces followed the Langmuir adsorption isotherm model.
5. Effect of Keto-enol tautomerism and different possible conformational isomers was demonstrated using DFT methods.